TECHNOMETRICS
2024, VOL. 66, NO. 4, 531–547
https://doi.org/10.1080/00401706.2024.2327346

Robust Multivariate Functional Control Chart

Christian Capezza, Fabio Centofanti, Antonio Lepore, and Biagio Palumbo

Department of Industrial Engineering, University of Naples Federico II, Naples, Italy

ABSTRACT

In modern Industry 4.0 applications, a huge amount of data is acquired during manufacturing processes and is often contaminated with outliers, which can seriously reduce the performance of control charting procedures, especially in complex and high-dimensional settings. In the context of profile monitoring, we propose a new framework that is referred to as robust multivariate functional control chart (RoMFCC) to monitor a multivariate functional quality characteristic while being robust to both functional casewise and componentwise outliers. In the former case, observations of the quality characteristic are contaminated in all functional variables or components, while, in the latter, the contamination affects one or more components independently. The RoMFCC relies on (I) a functional filter to identify componentwise outliers to be replaced by missing components; (II) a robust multivariate functional data imputation method; (III) a casewise robust dimensionality reduction; (IV) a monitoring strategy for the quality characteristic. Through a Monte Carlo simulation study, the RoMFCC is compared with competing schemes that have already appeared in the literature. A case study is finally presented where the proposed framework is used to monitor a resistance spot welding process in the automotive industry. RoMFCC is implemented in the R package funcharts, available online on CRAN.

ARTICLE HISTORY
Received January 2023
Accepted March 2024

KEYWORDS
Casewise and componentwise outliers; Functional data analysis; Profile monitoring; Robust estimation; Statistical process control

1. Introduction

Control charts are known as the main tools for statistical process monitoring (SPM), whose aim is to detect when a process is out of control (OC), or, equivalently, when special causes of variation act on it. In contrast, when only common causes are present, the process is said to be in control (IC). The current Industry 4.0 framework is however reshaping the format of measurements that can be gathered in manufacturing processes and calls for SPM applications able to deal massive amounts of data collected at high frequency by modern data acquisition systems.

In many cases, experimental measurements of the quality characteristic of interest are, in fact, characterized by complex and high-dimensional formats that are best represented by functional data (Ramsay and Silverman 2005; Kokoszka and Reimherr 2017), also referred to as profiles. The simplest approach in these cases is based on the extraction of scalar features from each profile and the application of classical multivariate SPM techniques (Montgomery 2012). However, the feature extraction step is known to be problem-specific, arbitrary, and possibly masking useful information. Thus, these issues stimulated a growing interest in *profile monitoring* (Noorossana, Saghaei, and Amiri 2011) that does not need an explicit feature extraction and can be directly applied to quality characteristics in the form of multiple profiles, also referred to as multivariate functional quality characteristics. Some recent examples can be found in Menafoglio et al. (2018), Capezza et al. (2020, 2021a, 2021b, 2023), and Centofanti et al. (2021, 2022).

Control charts are currently implemented in two phases. The first is referred to as Phase I and is concerned with the identification of a clean dataset to be assumed as representative of the IC state of the process, named Phase I sample or Phase I observations. Whereas, the second is referred to as Phase II and is concerned with prospective process monitoring, that is, the monitoring of future observations. Unfortunately, the identification of a Phase I sample in high-dimensional contexts is not an easy task, because of the large presence of outliers in at least one component of a multivariate functional quality characteristic. On the other hand, control charts are very sensitive to the presence of outliers in the Phase I sample as they inflate control limits and reduce the detection power in Phase II.

As a practical situation, let us consider the case study in the SPM of a resistance spot welding (RSW) process in automotive body-in-white manufacturing that will be thoroughly presented in Section 5. RSW is the most common technique employed in joining metal sheets, mainly because it guarantees the structural integrity and solidity of welded items while being adaptable for mass production (Martín et al. 2014). Among the online measurements of the parameters of the RSW process, the so-called dynamic resistance curve (DRC) shows how the electrical resistance between two pieces of metal being joined, measured in $m\Omega$, changes over time during the welding operation and is recognized as the complete technological signature of the metallurgical development of a spot weld (Dickinson et al. 1980; Capezza et al. 2021b). Being routinely performed on all spot

CONTACT Fabio Centofanti *fabio.centofanti@unina.it* Department of Industrial Engineering, University of Naples Federico II, Piazzale Tecchio 80, 80125, Naples, Italy.

Supplementary materials for this article are available online. Please go to *www.tandfonline.com/r/TECH*.

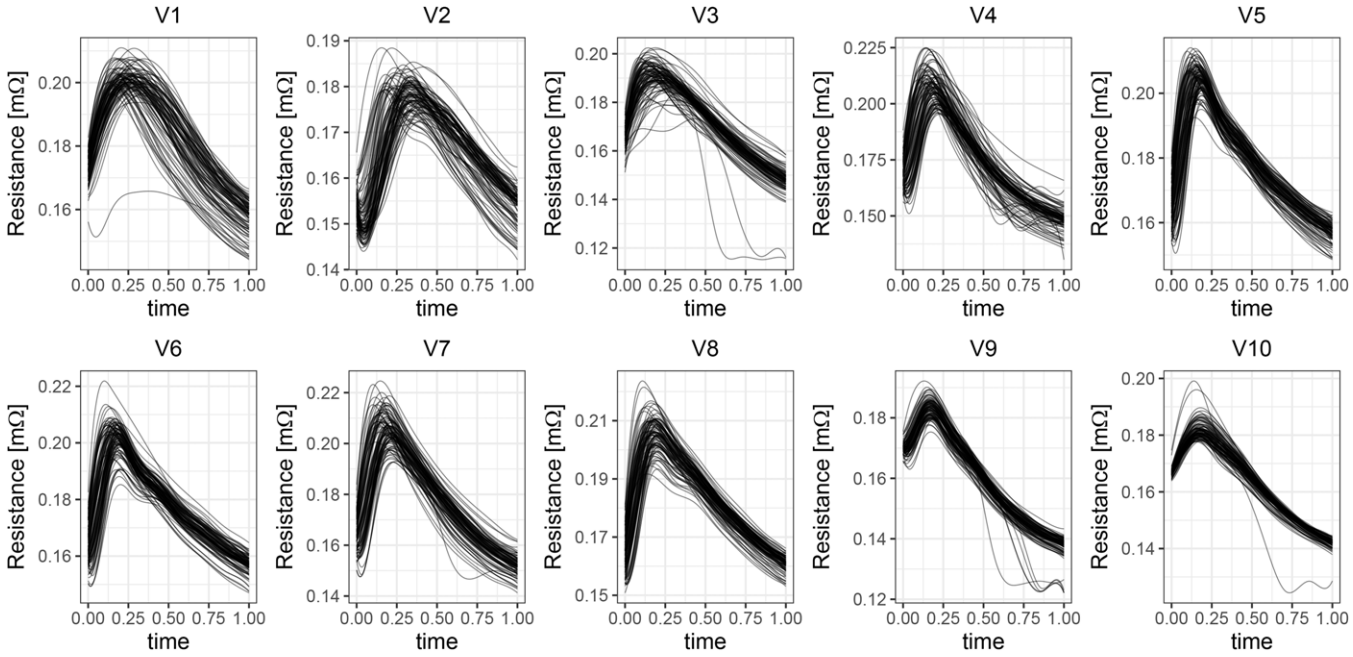

Figure 1. Sample of 100 DRCs, measured in $m\Omega$, that are acquired during the RSW process from the case study in Section 5. The different panels refer to the corresponding different spot welds, denoted with names from V1 to V10.

welds, it can be regarded as an in-line low-cost proxy of the RSW process quality concerning off-line costly destructive tests, which are performed only on a very small fraction of randomly selected items. In the dataset used for this case study and thoroughly described in Section 5, DRCs are acquired during RSW lab tests at Centro Ricerche Fiat (Italy) on different items, that is, car bodies, of the same model. Figure 1 shows 10 panels of DRCs, where each panel corresponds to a specific welding point on an item. For illustrative simplicity, each panel shows only 100 DRCs randomly sampled from the complete dataset used in Section 5, corresponding to as many different items. Figure 1 clearly highlights the motivating challenge of handling outliers for each item, possibly occurring in a few components (i.e., panels), or all of them, due to different inconvenient factors that may affect the final quality of a welded joint. One known factor is the expulsion of welded material that can occur in isolated weld spots due to excessive welding current and may be independent of other spots on the same item. This factor leads to an abrupt decline in the corresponding components of the multivariate DRCs. On the other hand, in case, in a situation where the RSW fails, or because of faulty measurement instrument calibration, all 10 points of the same item may have issues.

To deal with outliers, SPM methods use two common alternatives, namely the *diagnostic* and the *robust* approaches (Kruger and Xie 2012; Hubert, Rousseeuw, and Segaert 2015). The diagnostic approach is based on the removal of sample units identified as outliers and iterative re-estimation procedures in Phase I. This approach could be often safely applied to eliminate the effect of a small number of very extreme observations in the Phase I sample. However, it may fail in the detection of moderate outliers that may not be easy to label. On the contrary, the robust approach accepts all data points in Phase I and, by means of a robust estimator, reduces the impact of outliers on the final results (Maronna et al. 2019). It is worth explicitly noting that, throughout this article, the term *robust* means "outlier resistant" and not "robust to model misspecification." Moreover, under the robust approach, the terms Phase I sample or Phase I observations will still be used to refer to a dataset that is representative of the IC state even if possibly contaminated by outliers.

In the SPM literature, several robust approaches have been proposed for the monitoring of a multivariate scalar quality characteristic. Alfaro and Ortega (2009) show a comparison of robust alternatives to the classical Hotelling's T^2 control chart. They include two alternative Hotelling's T^2-type control charts for individual observations, proposed by Vargas (2003) and Jensen, Birch, and Woodall (2007), based on the minimum volume ellipsoid and the minimum covariance determinant estimators (Rousseeuw 1984), respectively. Moreover, the comparison includes the control chart based on the reweighted minimum covariance determinant estimators, proposed by Chenouri, Steiner, and Variyath (2009). More recently, Cabana and Lillo (2022) propose a robust Hotelling's T^2 procedure using the robust shrinkage reweighted estimator. To the best of the authors' knowledge, Kordestani et al. (2020) and Moheghi, Noorossana, and Ahmadi (2022) are the only ones to propose robust estimators to monitor simple linear profiles, which however are not able to capture more general nonlinear shapes such as the ones shown in Figure 1.

Beyond the SPM literature, several robust approaches have been proposed to deal with functional outliers. The classical L-estimator, which is the linear combination type estimator (Maronna et al. 2019), is extended to the functional data setting to robustly estimate the center of a functional distribution by trimming (Fraiman and Muniz 2001; Cuesta-Albertos and Fraiman 2006) and functional data depths (Cuevas and Fraiman 2009; López-Pintado and Romo 2011). In the same setting, Sinova, Gonzalez-Rodriguez, and Van Aelst (2018) introduce the notion of maximum-likelihood type estimator, referred to as M-estimator. More recently, Centofanti et al. (2023) propose a robust functional analysis of variance (ANOVA) to reduce

the weights of outlying functional data on the results of the analysis.

Robust approaches appeared also in functional principal component analysis (FPCA) and are classified by Boente and Salibián-Barrera (2021) in three groups, based on the specific property enjoyed by the resulting principal components. Methods in the first group perform the eigenanalysis of a robust estimator of the scatter operator, as the method of spherical principal components of Locantore et al. (1999) and the indirect approach of Sawant, Billor, and Shin (2012). The latter performs a robust PCA method (e.g., the ROBPCA proposed by Hubert, Rousseeuw, and Vanden Branden 2005) on the matrix of the basis coefficients corresponding to a basis expansion representation of the functional data. The second group contains projection-pursuit approaches as the one proposed by Hyndman and Ullah (2007), that sequentially search for the directions that maximize a robust estimator of the spread of the data projections. The third group consists of methods that estimate the principal component space by minimizing a robust reconstruction error measure (Lee, Shin, and Billor 2013). Additionally, it is worth mentioning diagnostic approaches for the detection of functional outliers for univariate (Hyndman and Shang 2010; Arribas-Gil and Romo 2014) and multivariate functional data (Hubert, Rousseeuw, and Segaert 2015; Ieva and Paganoni 2020; Alemán-Gómez et al. 2022). The reader is referred to supplementary material S4 of Capezza et al. (2023) for an extensive literature review on functional outlier detection methods and their software implementations.

In the presence of many functional variables or components, the curse of dimensionality exacerbates the development of scalable robust approaches. In fact, traditional multivariate robust estimators assume only a so-called *casewise* contamination model for the data, which consists of a mixture of two distributions, one representing the majority of cases that are free of contamination, and the second describing the minority of the cases assumed as generated by an unspecified outlier distribution. These traditional estimators work well when a small number of cases are contaminated. However, they are affected by the outlier propagation problem (Alqallaf et al. 2009) and may fail when the fraction of perfectly observed cases is small. Unfortunately, this is very common when the data are high-dimensional and outliers are *componentwise*, that is contamination in each variable is independent of the other ones.

Moreover, as pointed out by Agostinelli et al. (2015) in the multivariate scalar setting, casewise and componentwise data contamination may occur together. To overcome this problem, they propose a two-step method. In the first step, they use a univariate filter to detect large componentwise outliers and replace them with missing values. Then, to overcome the casewise contamination in the second step, a robust estimation specifically designed to deal with missing data is applied to the incomplete data. Leung, Yohai, and Zamar (2017) notice however that the univariate filter does not satisfactorily handle moderate-size componentwise outliers and introduce a consistent bivariate filter in combination with the univariate filter in the first step of Agostinelli et al. (2015). Rousseeuw and Bossche (2018) propose a new method for detecting deviating data cells that takes into account variables correlation, while Tarr, Müller, and Weber (2016) devise a method for robust estimation of precision matrices under componentwise contamination.

In this article, we propose a new framework, referred to as robust multivariate functional control chart (RoMFCC), for the SPM of multivariate functional data that is robust to both functional casewise and componentwise outliers. Mathematical definitions of the functional componentwise and casewise contamination models are provided in Section 2. The proposed framework is detailed in Section 3 and deals with functional componentwise outliers by introducing (i) an extension of the filtering approach proposed by Agostinelli et al. (2015) and Leung, Yohai, and Zamar (2017) for functional data; (ii) an imputation method inspired by the robust imputation technique of Branden and Verboven (2009); (iii) a robust multivariate functional principal component analysis (RoMFPCA) based on the ROBPCA method (Hubert, Rousseeuw, and Vanden Branden 2005); and (iv) a profile monitoring strategy built on the Hotelling's T^2 and the squared prediction error (*SPE*) control charts (Noorossana, Saghaei, and Amiri 2011; Grasso et al. 2016; Centofanti et al. 2021; Capezza et al. 2020, 2021a, 2023). The novelty of the proposed RoMFCC lies not only in each of these characteristic features, which are new in the functional data setting, but also in their combination with a general framework for the SPM of multivariate functional quality characteristics in the presence of casewise and componentwise outliers.

A Monte Carlo simulation study is performed in Section 4 to compare the RoMFCC with competing monitoring schemes that already appeared in the literature in terms of the ability to detect a process mean shift in Phase II, where the Phase I sample is contaminated by casewise and componentwise outliers in different scenarios. The practical applicability of the proposed control chart is illustrated in Section 5 through the motivating case study introduced above. Section 6 concludes the article. Supplementary materials are available online and contain details on data generation in the simulation study and additional simulation results. All computations and plots have been obtained using the programming language R (R Core Team 2021). The method presented in this article is implemented in the R package funcharts, openly available on CRAN (Capezza et al. 2024).

2. Functional Casewise and Componentwise Contamination Models

In this section, the functional casewise and componentwise contamination models are defined extending the definition of Alqallaf et al. (2009). Let $L^2(\mathcal{T})$ denote the Hilbert space of square-integrable functions defined on the compact set $\mathcal{T} \subset \mathbb{R}$, with the inner product of two functions $f, g \in L^2(\mathcal{T})$ given by $\langle f, g \rangle = \int_{\mathcal{T}} f(t)\, g(t)\, dt$, and the norm $\|\cdot\| = \sqrt{\langle \cdot, \cdot \rangle}$. Let the multivariate functional quality characteristic $\boldsymbol{X} = \left(X_1, \ldots, X_p\right)^T$ be a random vector with realizations in the Hilbert space $\mathbb{H}$ of p-dimensional vectors of $L^2(\mathcal{T})$ functions, with the inner product of two function vectors $\boldsymbol{f} = \left(f_1, \ldots, f_p\right)^T$ and $\boldsymbol{g} = \left(g_1, \ldots, g_p\right)^T$ in $\mathbb{H}$ given by $\langle \boldsymbol{f}, \boldsymbol{g} \rangle_{\mathbb{H}} = \sum_{j=1}^{p} \langle f_j, g_j \rangle$ and the norm $\|\cdot\|_{\mathbb{H}} = \sqrt{\langle \cdot, \cdot \rangle_{\mathbb{H}}}$. Let us assume that $\boldsymbol{X}$ is generated using the following model.

$$\boldsymbol{X} = (\boldsymbol{I} - \boldsymbol{B})\, \boldsymbol{Y} + \boldsymbol{B}\boldsymbol{Z}, \tag{1}$$

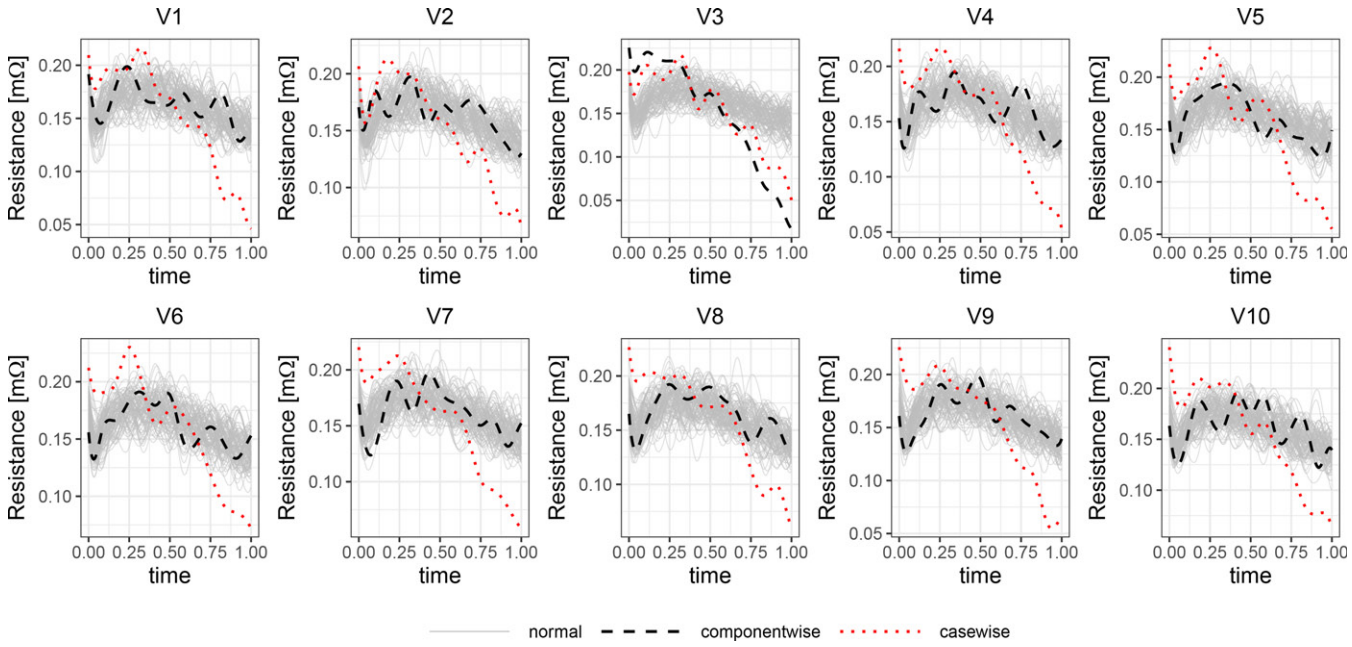

Figure 2. Sample of 100 observations of a multivariate functional quality characteristic, free of contamination, plotted as gray solid lines, simulated according to Section 4, which try to mimic the DRCs behavior in Figure 1, with two additional observations affected by functional componentwise and casewise contamination, plotted with dashed and dotted lines, respectively.

where $\boldsymbol{B} = \text{diag}(B_1, \ldots, B_p)$ is a diagonal matrix whose entries are Bernoulli random variables with $P(B_i = 1) = \epsilon_i$, $\boldsymbol{Z} \in \mathbb{H}$ has an arbitrary and unspecified outlier generating distribution, and $\boldsymbol{Y} \in \mathbb{H}$ follows a given distribution that represents the generating process free of any contamination. As in Alqallaf et al. (2009), we restrict our attention to the simpler case where $\boldsymbol{Y}, \boldsymbol{B}$ and $\boldsymbol{Z}$ are independent. Various contamination models arise from different assumptions about the joint distribution of $B_1, \ldots, B_p$. When these variables are fully dependent, that is, $P\left(B_1 = \cdots = B_p\right) = 1$, Equation (1) simplifies to the *functional casewise contamination model*. In this model, the probability that a given observation of a multivariate quality characteristic is not contaminated is $1 - \epsilon$, independently of the dimension p. That is, a given observation of a multivariate quality characteristic can be either contaminated in all components or not contaminated at all. On average, we expect a fraction $1-\epsilon$ of observations to be perfectly observed. However, the functional casewise contamination model, which is independent of p, is unrealistic when p is relatively large with respect to the number of realizations of $\boldsymbol{X}$. On the contrary, when p is relatively small, down-weighting the influence of suspicious cases can be an effective strategy.

At the other end, when $B_1, \ldots, B_p$ are independent, Equation (1) gives rise to the *functional componentwise contamination model*. As an example, let us suppose that $P(B_1 = 1) = \cdots = P\left(B_p = 1\right) = \epsilon$. Then, the probability $(1 - \epsilon)^p$ that a case is perfectly observed under this model quickly decreases with p and goes below 0.5 as p increases.

Figure 2 shows in grey a sample of 100 observations of a multivariate functional quality characteristic with $p = 10$ components, which are free of contamination and are simulated as described in Section 4 to mimic the behavior of the DRCs in the case study dataset already shown in Figure 1. Two additional observations affected by functional componentwise and casewise contamination are superimposed on Figure 2, and plotted in dashed and dotted lines, respectively. While for the latter all the components are contaminated, in the former only the third component (V3) is contaminated. If the multivariate functional quality characteristic is distributed according to the componentwise contamination model with a very low value of ϵ, say 0.05, nearly 60% of the observations are contaminated, and therefore, standard casewise robust functional methods would break down providing unsatisfactory results. On the contrary, when data follow the functional casewise contamination model, a standard casewise robust functional method would be more appropriate because componentwise approaches are known to perform poorly against this type of outliers (Alqallaf et al. 2009; Maronna et al. 2019).

Unfortunately, in practice, both casewise and componentwise functional outliers often occur simultaneously. That is, there are some observations fully spoiled (as in the functional casewise contamination model) and some others having components independently contaminated (as in the functional componentwise contamination model). In this case, a method, as the proposed one, that is able to simultaneously take into account both types of contamination is expected to provide better solutions to scenarios where the $B_1, \ldots, B_p$ are neither independent of each other nor fully dependent with respect to methods designed to be robust against either casewise or componentwise contamination models alone. Additional results in supplementary materials C further demonstrate the need to be robust against both types of outliers.

3. The Robust Multivariate Functional Control Chart Framework

The proposed RoMFCC is a new general framework for the SPM of multivariate functional data and is able to deal with both

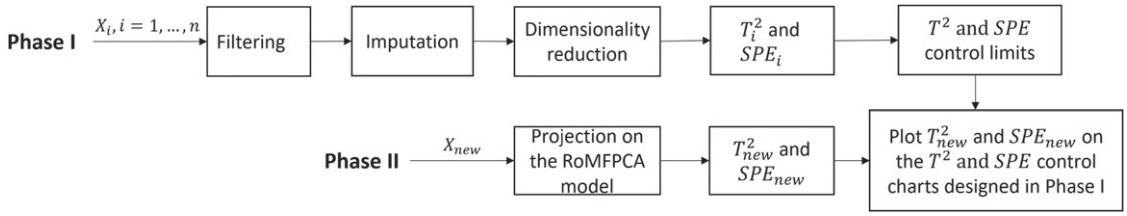

Figure 3. Scheme of the RoMFCC framework.

Phase I functional casewise and componentwise outliers. It is based on the following four main elements:

(I) a *functional filter* to identify functional componentwise outliers and replace them with missing component values;
(II) a *robust multivariate functional data imputation* to replace missing values;
(III) a *casewise robust dimensionality reduction* to reduce the infinite dimensionality of the multivariate functional data that is robust to casewise outliers;
(IV) a *monitoring strategy* to be applied on the multivariate functional quality characteristic as obtained after the previous steps.

These elements are combined in the proposed RoMFCC framework in a Phase II monitoring strategy described in the scheme of Figure 3, where a set of Phase I observations $\boldsymbol{X}_i$, $i = 1, \ldots, n$ of the multivariate functional quality characteristic $\boldsymbol{X}$, which can be contaminated by outliers, is used for the design of the control chart. In what follows, we describe a specific implementation of the RoMFCC framework. In the *filtering* step, we propose a (I) functional filter, which is named FF and is an extension of the filtering stage of Agostinelli et al. (2015) and Leung, Yohai, and Zamar (2017) that aims to identify functional componentwise outliers and replace them with missing components. The latter are then imputed through a new (II) *robust multivariate functional data imputation*, which is named RoMFDI and is a functional extension of the technique of Branden and Verboven (2009). The imputed Phase I sample so obtained is used to estimate the RoMFPCA model, which in turn is used for the (III) *casewise robust dimensionality reduction* step. The Hotelling's T^2 and *SPE* control charts are then used as (IV) *monitoring strategy*. In Phase II, each new observation $\boldsymbol{X}_{new}$ is projected on the RoMFPCA model to compute the values of Hotelling's T^2 and *SPE* statistics according to the model identified in Phase I and referred to as T_{new}^2 and SPE_{new}, respectively. An alarm signal is issued if either T_{new}^2 or SPE_{new} violates the corresponding control limit.

The methods used in the filtering, imputation, and dimensionality reduction steps are completely new in both the functional and profile monitoring literature. Specifically, the FF is a novel extension to the functional setting of the methods presented in Agostinelli et al. (2015) and Leung, Yohai, and Zamar (2017) for multivariate non-functional data. The RoMFDI approach is the first imputation technique for functional missing data that uses the idea of Branden and Verboven (2009). Finally, although robust dimensionality reduction methods have appeared for univariate functional data, RoMFPCA is the first casewise robust method for multivariate functional quality characteristics. In addition to innovation in each of these characteristic features, the novelty of the proposed RoMFCC lies also in their combination in a whole monitoring procedure through the nontrivial implementation pipeline outlined in Figure 3. Indeed, its modularity is imposed to the extent of setting up a framework as broad as possible for the process monitoring of a multivariate functional quality characteristic in the presence of casewise and componentwise outliers. On the contrary, the use of the T^2 and *SPE* control charts as a monitoring strategy is instead a standard profile monitoring technique (Centofanti et al. 2021; Capezza et al. 2023) and is the only element of the proposed method that has already appeared in the literature, even if, thanks to the modularity imposed on the proposed framework, it can be, in principle, replaced by a more sophisticated approach.

Moreover, to prevent overfitting issues that could reduce the monitoring performance of the RoMFCC when the sample size n is small compared to the number of process variables (Ramaker et al. 2004; Kruger and Xie 2012), the Phase I sample is randomly split into nonoverlapping sets, referred to as *training* and *tuning* sets. The former is used to estimate the RoMFPCA model, whereas the latter is considered to estimate the T^2 and *SPE* control limits.

The RoMFPCA is presented in Section 3.1. Then, the FF, the RoMFDI method, and the monitoring strategy are described in Sections 3.2–3.4, respectively.

3.1. Robust Multivariate Functional Principal Component Analysis

We assume that $\boldsymbol{X}$ has mean $\boldsymbol{\mu} = \left(\mu_1, \ldots, \mu_p\right)^T$, where $\mu_j(t) = \mathrm{E}(X_j(t))$, $j = 1, \ldots, p$, $t \in \mathcal{T}$ and covariance $\boldsymbol{G} = \{G_{jk}\}_{1 \le j,k \le p}$, $G_{jk}(s,t) = \mathrm{cov}(X_j(s), X_k(t))$, $s, t \in \mathcal{T}$. Differences in variability and unit of measurement among $X_1, \ldots, X_p$ are taken into account using the transformation approach of Chiou, Chen, and Yang (2014), that is, we replace $\boldsymbol{X}$ with its standardized version $\boldsymbol{Z} = \left(Z_1, \ldots, Z_p\right)^T$, where $Z_j(t) = v_j(t)^{-1/2}(X_j(t) - \mu_j(t))$, with $v_j(t) = G_{jj}(t,t)$, $j = 1, \ldots, p$, $t \in \mathcal{T}$. From the multivariate Karhunen-Loève's theorem (Happ and Greven 2018) it follows that

$$\boldsymbol{Z}(t) = \sum_{l=1}^{\infty} \xi_l \boldsymbol{\psi}_l(t), \quad t \in \mathcal{T},$$

where $\xi_l = \langle \boldsymbol{\psi}_l, \boldsymbol{Z} \rangle_{\mathbb{H}}$ are random variables, say *principal components scores* or simply *scores*, such that $\mathrm{E}(\xi_l) = 0$ and $\mathrm{E}(\xi_l \xi_m) = \lambda_l \delta_{lm}$, with δ_{lm} the Kronecker delta. The elements of the orthonormal set $\{\boldsymbol{\psi}_l\}$, $\boldsymbol{\psi}_l = \left(\psi_{l1}, \ldots, \psi_{lp}\right)^T$, with $\langle \boldsymbol{\psi}_l, \boldsymbol{\psi}_m \rangle_{\mathbb{H}} = \delta_{lm}$, are referred to as *principal components*, and

are the eigenfunctions of the covariance $\boldsymbol{C}$ of $\boldsymbol{Z}$ corresponding to the eigenvalues $\lambda_1 \geq \lambda_2 \geq \cdots \geq 0$. As in the approach of Ramsay and Silverman (2005), the eigenfunctions and eigenvalues of the covariance $\boldsymbol{C}$ are estimated through a basis function expansion approach. Specifically, we assume that, for $j = 1, \ldots, p$, $l = 1, \ldots, \infty$, Z_j and ψ_{lj} can be approximated by the following finite sums of K terms

$$Z_j(t) \approx \sum_{k=1}^{K} c_{jk}\phi_{jk}(t), \quad \psi_{lj}(t) \approx \sum_{k=1}^{K} b_{ljk}\phi_{jk}(t), \quad t \in \mathcal{T}. \quad (2)$$

That is, Z_j and ψ_{lj} are approximated by a linear combination of the components of a K-dimensional vector of basis functions $\boldsymbol{\phi}_j = \left(\phi_{j1}, \ldots, \phi_{jK}\right)^T$, with coefficient vectors $\boldsymbol{c}_j = \left(c_{j1}, \ldots, c_{jK}\right)^T$ and $\boldsymbol{b}_{lj} = \left(b_{lj1}, \ldots, b_{ljK}\right)^T$, respectively. With these assumptions, the standard multivariate functional principal component analysis (Ramsay and Silverman 2005; Chiou, Chen, and Yang 2014) estimates the eigenfunctions and eigenvalues of the covariance $\boldsymbol{C}$ by performing the standard multivariate principal component analysis on the random vector $\boldsymbol{W}^{1/2}\boldsymbol{c}$, where $\boldsymbol{c} = \left(\boldsymbol{c}_1^T, \ldots, \boldsymbol{c}_p^T\right)^T$ and $\boldsymbol{W}$ is a block-diagonal matrix with diagonal blocks $\boldsymbol{W}_j$, $j = 1, \ldots, p$, whose entries are $\langle \phi_{jk_1}, \phi_{jk_2} \rangle$, $k_1, k_2 = 1, \ldots, K$. Then, the eigenvalues λ_l of $\boldsymbol{C}$ are estimated by those of the covariance matrix of $\boldsymbol{W}^{1/2}\boldsymbol{c}$, while the components $\psi_{l1}, \ldots, \psi_{lp}$ of the corresponding eigenfunction $\boldsymbol{\psi}_l$ are estimated by (2) with $\boldsymbol{b}_{lj} = \boldsymbol{W}^{-1/2}\boldsymbol{u}_{lj}$, where $\boldsymbol{u}_l = \left(\boldsymbol{u}_{l1}^T, \ldots, \boldsymbol{u}_{lp}^T\right)^T$ is the eigenvector of the covariance matrix of $\boldsymbol{W}^{1/2}\boldsymbol{c}$ corresponding to λ_l. It is well known that the standard multivariate principal component analysis is not robust to outliers (Maronna et al. 2019) and this obviously reflects the functional principal component analysis. Extending the approach of Sawant, Billor, and Shin (2012) for multivariate functional data, the proposed RoMFPCA applies a robust alternative of the principal component analysis to the random vector $\boldsymbol{W}^{1/2}\boldsymbol{c}$, through the ROBPCA approach of Hubert, Rousseeuw, and Vanden Branden (2005), which is a computationally efficient method explicitly conceived to produce estimates with high breakdown in high-dimensional data settings and is commonly adopted in the functional context to handle a large percentage of contamination. Thus, given n independent realizations $\boldsymbol{X}_1, \ldots, \boldsymbol{X}_n$ of $\boldsymbol{X}$, dimensionality reduction is achieved by approximating $\boldsymbol{X}_i$ through $\hat{\boldsymbol{X}}_i$, for $i = 1, \ldots, n$, as

$$\hat{\boldsymbol{X}}_i(t) = \hat{\boldsymbol{\mu}}(t) + \hat{\boldsymbol{D}}(t) \sum_{l=1}^{L} \hat{\xi}_{il}\hat{\boldsymbol{\psi}}_l(t) \quad t \in \mathcal{T}, \quad (3)$$

where $\hat{\boldsymbol{D}}$ is a diagonal matrix whose diagonal entries are robust estimates $\hat{\nu}_j^{1/2}$ of $\nu_j^{1/2}$, $\hat{\boldsymbol{\mu}} = \left(\hat{\mu}_1, \ldots, \hat{\mu}_p\right)^T$ is a robust estimate of $\boldsymbol{\mu}$, $\hat{\boldsymbol{\psi}}_l$, $l = 1, \ldots, L$, are the first L robustly estimated principal components and $\hat{\xi}_{il} = \langle \hat{\boldsymbol{\psi}}_l, \hat{\boldsymbol{Z}}_i \rangle_{\mathbb{H}}$ are the corresponding scores with robustly estimated variances $\hat{\lambda}_l$. Estimates $\hat{\boldsymbol{\psi}}_l$ and $\hat{\lambda}_l$ are obtained through the n realizations of $\boldsymbol{Z}_i$ estimated as $\hat{\boldsymbol{Z}}_i = \hat{\nu}_j^{-1/2}(\boldsymbol{X}_i - \hat{\boldsymbol{\mu}}_i)$ by using $\hat{\mu}_j$ and $\hat{\nu}_j$. The robust estimates $\hat{\mu}_j$ and $\hat{\nu}_j$ are obtained through the scale equivariant functional M-estimator and the functional normalized median absolute deviation estimator proposed by Centofanti et al. (2023), whose details are provided in supplementary materials A. As in the multivariate setting, L is generally chosen such that the retained principal components $\hat{\boldsymbol{\psi}}_1, \ldots, \hat{\boldsymbol{\psi}}_L$ explain at least a given percentage, say 70%–90%, of total variability. However, more sophisticated methods could also be used (see Jolliffe 2011 for additional details).

3.2. Functional Filter

To extend the filter of Agostinelli et al. (2015) and Leung, Yohai, and Zamar (2017) to univariate functional data, let us consider n independent realizations $\boldsymbol{X}_i = \left(X_{i1}, \ldots, X_{ip}\right)^T$, $i = 1, \ldots, n$, of the multivariate functional quality characteristic $\boldsymbol{X}$. The FF is based on the sequential application of univariate and bivariate filters. For each jth component, $j = 1, \ldots, p$, the univariate filter considers the functional distances

$$D_{ij}^{\text{fil}} = \sum_{l=1}^{L^{\text{fil}}} \frac{(\hat{\xi}_{ijl}^{\text{fil}})^2}{\hat{\lambda}_{jl}^{\text{fil}}}, \quad i = 1, \ldots, n, \quad (4)$$

where the estimated scores $\hat{\xi}_{ijl}^{\text{fil}} = \langle \hat{\psi}_{jl}^{\text{fil}}, \hat{Z}_{ij} \rangle$, eigenvalues $\hat{\lambda}_{lj}^{\text{fil}}$, principal components $\hat{\psi}_{lj}^{\text{fil}}$, and standardized observations $\hat{Z}_{ij}$ of X_{ij} are obtained by applying, with $p = 1$, the proposed RoMFPCA described in Section 3.1 to the sample $X_{1j}, \ldots, X_{nj}$. In this setting, RoMFPCA is suitable for representing distances among X_{ij}'s and not for performing dimensionality reduction, thus, L^{fil} should be sufficiently large to capture a large fraction δ^{fil} of total variability. Let G_n be the empirical cdf of D_{ij}^{fil}, that is,

$$G_n(x) = \frac{1}{n} \sum_{i=1}^{n} I(D_{ij}^{\text{fil}} \leq x), \quad x \geq 0,$$

where $I(\cdot)$ denotes the indicator function. Then, X_{ij} is labeled as a componentwise outlier by comparing $G_n(x)$ with $G(x)$, $x \geq 0$, where G is the reference cdf for D_{ij}^{fil}. Following Leung, Yohai, and Zamar (2017), we consider D_{ij}^{fil} distributed as a Chi-squared random variable with L^{fil} degrees of freedom, in short $D_{ij}^{\text{fil}} \sim \chi^2_{L^{\text{fil}}}$. The proportion of flagged componentwise outliers is defined by

$$d_n = \sup_{x \geq \eta} \{G(x) - G_n(x)\}^+,$$

where $\{a\}^+$ represents the positive part of a, and $\eta = G^{-1}(\alpha)$ is a large quantile of D_{ij}^{fil}. As Agostinelli et al. (2015), we set $\alpha = 0.95$. Finally, we flag $\lfloor n d_n \rfloor$ observations with the largest functional distances D_{ij}^{fil} as functional componentwise outliers, where $\lfloor \cdot \rfloor$ denotes the floor function.

From the arguments presented by Agostinelli et al. (2015) and Leung, Yohai, and Zamar (2017), the proposed FF is consistent even when the actual distribution of D_{ij}^{fil} is unknown. That is, when the tail of G is heavier than or equal to that of the actual unknown distribution, it will flag a componentwise outlier asymptotically correctly. This result is formally stated in the following Proposition 1, whose proof is deferred to supplementary materials B.

Proposition 1. Let $D_{i,j}^{\text{fil}} \xrightarrow{d} D_0 \sim G_0$, where G_0 is assumed to be a continuous distribution. If the reference distribution G satisfies

$$\sup_{x \geq \eta} \{G(x) - G_0(x)\} \leq 0, \tag{5}$$

then

$$\frac{n_0}{n} \to 0 \quad a.s.,$$

where $n_0 = \lfloor n d_n \rfloor$.

Note that the missing data created in the filtering step are not missing at random because they depend on the original data. However, in case of no contamination, if each component X_i of the multivariate functional quality characteristic $\boldsymbol{X}$ is distributed such that the asymptotic distribution G_0 of D_{ij}^{fil} satisfies (5), then the proportion of casewise outliers and thus missing components converges to zero. Hence, the filtering step does not affect the consistency property of the estimator in the dimensionality reduction step because no functional componentwise outlier is identified.

On top of this univariate filter, as done by Leung, Yohai, and Zamar (2017) in the multivariate scalar setting, a bivariate filter is applied to take into account the correlation across the different components. Let $\boldsymbol{U}$ be the resulting $n \times p$ auxiliary matrix with elements U_{ij} that can be either zero, indicating the filtered components in $\boldsymbol{X}_1, \ldots, \boldsymbol{X}_n$, or one. Then, let us apply a filtering strategy on all pairs of components $1 \leq j < k \leq p$ of $\boldsymbol{X}_i$, $i = 1, \ldots, n$, to identify outlying bivariate functions to filter the moderately contaminated components, that is, not flagged by the univariate filter. For a pair of components (X_{ij}, X_{ik}), let us set $\boldsymbol{X}_i^{(jk)} = (X_{ij}, X_{ik})$ and apply RoMFPCA to $\boldsymbol{X}_1^{(jk)}, \ldots, \boldsymbol{X}_n^{(jk)}$, which produces scores $\hat{\xi}_{il}^{\text{fil}(jk)}$ and eigenvalues $\hat{\lambda}_l^{\text{fil}(jk)}$, with $l \geq 1$. Then a bivariate filter is applied based on the pairwise distances $D_i^{(jk)} = \sum_{l=1}^{L^{\text{fil}(jk)}} (\hat{\xi}_{il}^{\text{fil}(jk)})^2 / \hat{\lambda}_l^{\text{fil}(jk)}$ calculated on the pairs (j,k) with no flagged components in the univariate filtering step, that is, such that $U_{ij} = U_{ik} = 1$. The numbers of principal components retained $L^{\text{fil}(jk)}$ are chosen similarly to L^{fil} in (4). We apply this procedure to all pairs of components $1 \leq j < k \leq p$. Let $J = \{(i,j,k) : D_i^{(j,k)}$ is flagged as bivariate outlier$\}$ be the set of triplets that identify the pairs (j,k) of components flagged by the bivariate filter in observations $i = 1, \ldots, n$. It remains to determine which components (i,j) of the ith observation should be flagged as componentwise outliers. For each component (i,j), $i = 1, \ldots, n$, $j = 1, \ldots, p$, we count the number of pairs flagged in the ith observation where the component (i,j) is involved as $m_{ij} = \#\{k : (i,j,k) \in J\}$. Cells with large m_{ij} are likely to correspond to univariate functional outliers. In case of no contamination, m_{ij} approximately follows the binomial distribution $Bin(\sum_{k \neq j} U_{ik}, \delta)$, where δ is the overall proportion of componentwise outliers that are not detected by the univariate filter. We flag X_{ij} as componentwise outlier if $m_{ij} > c_{ij}$, where c_{ij} is the 0.99-quantile of $Bin(\sum_{k \neq j} U_{ik}, \delta)$. In practice, following Leung, Yohai, and Zamar (2017), we recommend the conservative choice $\delta = 0.10$. The benefits of using the bivariate filter in conjunction with the univariate filter are assessed in supplementary materials C.

3.3. Robust Multivariate Functional Data Imputation

Let us consider the setting where the n independent realizations $\boldsymbol{X}_i = \left(X_{i1}, \ldots, X_{ip}\right)^T$, $i = 1, \ldots, n$ of the multivariate functional quality characteristic $\boldsymbol{X}$ may present missing components, that is, for some i, at least one among $X_{i1}, \ldots, X_{ip}$ is missing. Let us assume that there is a set S_c of $c < n$ realizations without missing components. As the robust imputation approach of Branden and Verboven (2009), the RoMFDI is a sequential imputation method. It starts from a realization $\boldsymbol{X}_{\underline{i}} \notin S_c$ having the smallest number, say s, of missing components. For convenience in notation and without loss of generality, arrange the p components of $\boldsymbol{X}_{\underline{i}} = ((\boldsymbol{X}_{\underline{i}}^{\text{m}})^T, (\boldsymbol{X}_{\underline{i}}^{\text{o}})^T)^T$ such that the first s missing components are in the vector $\boldsymbol{X}_{\underline{i}}^{\text{m}}$, while the remaining $p - s$ observed ones are in $\boldsymbol{X}_{\underline{i}}^{\text{o}}$. The standardized version of $\boldsymbol{X}_{\underline{i}}$ is partitioned as $\hat{\boldsymbol{Z}}_{\underline{i}} = ((\hat{\boldsymbol{Z}}_{\underline{i}}^{\text{m}})^T, (\hat{\boldsymbol{Z}}_{\underline{i}}^{\text{o}})^T)^T$, where $\hat{\boldsymbol{Z}}_{\underline{i}}^{\text{m}}$ and $\hat{\boldsymbol{Z}}_{\underline{i}}^{\text{o}}$ are the standardized versions of $\boldsymbol{X}_{\underline{i}}^{\text{m}}$ and $\boldsymbol{X}_{\underline{i}}^{\text{o}}$, respectively. By (2), $\hat{\boldsymbol{Z}}_{\underline{i}}$ is uniquely identified by the (Kp)-dimensional coefficient vector $\boldsymbol{c}_{\underline{i}} = ((\boldsymbol{c}_{\underline{i}}^{\text{m}})^T, (\boldsymbol{c}_{\underline{i}}^{\text{o}})^T)^T$ related to the basis expansions of its p components, where K is the number of basis functions as in (2). Therefore, the imputation of $\boldsymbol{X}_{\underline{i}}^{\text{m}}$ reduces to the imputation of $\boldsymbol{c}_{\underline{i}}^{\text{m}}$. We do this by minimizing the distance of $\boldsymbol{X}_{\underline{i}}$ from the space generated by the realizations in S_c

$$\sum_{l=1}^{L^{\text{imp}}} \frac{(\hat{\xi}_{\underline{i}l}^{\text{imp}})^2}{\hat{\lambda}_l^{\text{imp}}}, \tag{6}$$

where $\hat{\xi}_{\underline{i}l}^{\text{imp}} = \langle \hat{\boldsymbol{\psi}}_l^{\text{imp}}, \hat{\boldsymbol{Z}}_{\underline{i}} \rangle_{\mathbb{H}}$, with principal components $\hat{\boldsymbol{\psi}}_l^{\text{imp}} = (\hat{\psi}_{l1}^{\text{imp}}, \ldots, \psi_{lp}^{\text{imp}})^T$ and corresponding eigenvalues $\hat{\lambda}_l^{\text{imp}}$ obtained by applying RoMFPCA on the complete realizations in S_c, as in Section 3.1. The number L^{imp} of components is chosen sufficiently large to capture the desired percentage of total variability δ^{imp}. Since the principal components $\hat{\psi}_{lj}^{\text{imp}}$ are uniquely identified by their basis coefficients $\hat{\boldsymbol{b}}_{lj}$, $l = 1, \ldots, L^{\text{imp}}$, $j = 1, \ldots, p$, which can be arranged in the matrix $\hat{\boldsymbol{B}}$ having columns $\hat{\boldsymbol{b}}_l = \left(\hat{\boldsymbol{b}}_{l1}^T, \ldots, \hat{\boldsymbol{b}}_{lp}^T\right)^T$, the objective function (6) can be calculated as $\boldsymbol{c}_{\underline{i}}^T \boldsymbol{C} \boldsymbol{c}_{\underline{i}}$, where the $Kp \times Kp$ matrix $\boldsymbol{C}$ is

$$\boldsymbol{C} = \boldsymbol{W} \hat{\boldsymbol{B}} \hat{\boldsymbol{\Lambda}}^{-1} \hat{\boldsymbol{B}}^T \boldsymbol{W} = \begin{pmatrix} \boldsymbol{C}^{\text{m,m}} & \boldsymbol{C}^{\text{m,o}} \\ (\boldsymbol{C}^{\text{m,o}})^T & \boldsymbol{C}^{\text{o,o}} \end{pmatrix},$$

with $\boldsymbol{W}$ denoting the block-diagonal matrix defined in Section 3.1 and $\hat{\boldsymbol{\Lambda}}$ the diagonal matrix with diagonal entries $\hat{\lambda}_l^{\text{imp}}$, $l = 1, \ldots, L^{\text{imp}}$. The upper left $Ks \times Ks$ block $\boldsymbol{C}^{\text{m,m}}$ of $\boldsymbol{C}$ contains the elements corresponding to the missing components, while $\boldsymbol{C}^{\text{m,o}}$ contains the elements with the missing components in the rows and the observed components in the columns. The solution that minimizes the objective function (6) with respect to $\boldsymbol{c}_{\underline{i}}^{\text{m}}$ is

$$\begin{aligned} \hat{\boldsymbol{c}}_{\underline{i}}^{\text{m}} &= \underset{\boldsymbol{c}_{\underline{i}}^{\text{m}}}{\text{argmin}} \left(\left(\boldsymbol{c}_{\underline{i}}^{\text{m}}\right)^T, \left(\boldsymbol{c}_{\underline{i}}^{\text{o}}\right)^T \right)^T \boldsymbol{C} \left(\left(\boldsymbol{c}_{\underline{i}}^{\text{m}}\right)^T, \left(\boldsymbol{c}_{\underline{i}}^{\text{o}}\right)^T \right) \\ &= -\left(\boldsymbol{C}^{\text{m,m}}\right)^+ \boldsymbol{C}^{\text{m,o}} \boldsymbol{c}_{\underline{i}}^{\text{o}}, \end{aligned} \tag{7}$$

where $(\boldsymbol{C}^{\text{m,m}})^+$ is the Moore-Penrose inverse of $\boldsymbol{C}^{\text{m,m}}$.

To overcome the correlation bias issue typical of deterministic imputation approaches (Van Buuren 2018; Little and Rubin 2019), we propose a stochastic imputation method by imputing $\boldsymbol{c}_{\underline{i}}^{\mathrm{m}}$ with

$$\boldsymbol{c}_{\underline{i}}^{\mathrm{imp}} = \hat{\boldsymbol{c}}_{\underline{i}}^{\mathrm{m}} + \boldsymbol{\varepsilon}_{\underline{i}}. \tag{8}$$

The last term $\boldsymbol{\varepsilon}_{\underline{i}}$ is a multivariate normal random variable with mean zero and covariance matrix robustly estimated (e.g., using the Rocke type estimator (Rocke 1996)) based on the regression residuals of the coefficient vectors of the missing component on those of the observed components, by using the observations in S_c through the model in (7). Accordingly, the components of $\hat{\boldsymbol{Z}}_{\underline{i}}^{\mathrm{m}}$ are imputed with $\hat{\boldsymbol{Z}}_{\underline{i}}^{\mathrm{imp}}$, whose jth component is

$$\hat{Z}_{\underline{i}j}^{\mathrm{imp}}(t) = \left(\boldsymbol{c}_{\underline{i}j}^{\mathrm{imp}}\right)^T \boldsymbol{\phi}_j(t), \quad t \in \mathcal{T}, \quad j = 1, \ldots, s,$$

where $\boldsymbol{c}_{\underline{i}j}^{\mathrm{imp}}$ is the vector of the elements of $\boldsymbol{c}_{\underline{i}}^{\mathrm{imp}}$ corresponding to the jth component of $\hat{\boldsymbol{Z}}_{\underline{i}}$ and $\boldsymbol{\phi}_j$ is defined as in (2). The imputed values of $\boldsymbol{X}_{\underline{i}}^{\mathrm{m}}$ are finally obtained by unstandardizing $\hat{\boldsymbol{Z}}_{\underline{i}}^{\mathrm{imp}}$, and $\boldsymbol{X}_{\underline{i}}$ is then added to S_c. The whole imputing step described for $\boldsymbol{X}_{\underline{i}}$ is repeated iteratively until all realizations with missing components are imputed. Realizations where all components are missing, that is, $s = p$, are trivially removed from the sample because their imputation does not provide any additional information for the analysis.

However, similarly to Branden and Verboven (2009), if the cardinality of S_c in the first iteration is sufficiently large, we suggest not updating the RoMFPCA model at each iteration. To take into account the increased noise due to single imputation, the proposed RoMFDI can be easily included in a multiple imputation framework (Van Buuren 2018; Little and Rubin 2019). Due to the presence of the stochastic component $\boldsymbol{\varepsilon}_{\underline{i}}$ in (8), it is worth explicitly noting that the imputed dataset is not deterministically assigned. Therefore, by performing several times the RoMFDI in the imputation step of the RoMFCC implementation, the corresponding multiple estimated RoMFPCA models could be combined by averaging the robustly estimated covariance functions, thus, performing a multiple imputation strategy as suggested by Van Ginkel et al. (2007). In supplementary materials C, the proposed RoMFDI method performance is assessed against simple case deletion and mean imputation.

3.4. The Monitoring Strategy

The last (IV) element of the proposed RoMFCC implementation relies on the consolidated monitoring strategy for a multivariate functional quality characteristic $\boldsymbol{X}$ based on Hotelling's T^2 and *SPE* control charts. The former assesses the stability of $\boldsymbol{X}$ in the finite-dimensional space spanned by the first principal components identified through the RoMFPCA (Section 3.1), while the latter monitors changes along directions in its orthogonal complement space. Specifically, the Hotelling's T^2 statistic for $\boldsymbol{X}$ is defined as

$$T^2 = \sum_{l=1}^{L^{\mathrm{mon}}} \frac{(\xi_l^{\mathrm{mon}})^2}{\lambda_l^{\mathrm{mon}}},$$

where λ_l^{mon} are the variances of the scores $\xi_l^{\mathrm{mon}} = \langle \boldsymbol{\psi}_l^{\mathrm{mon}}, \boldsymbol{Z} \rangle_{\mathbb{H}}$, $\boldsymbol{Z}$ is the standardized version of $\boldsymbol{X}$ as defined in Section 3.1 and $\boldsymbol{\psi}_l^{\mathrm{mon}}$ is the vector of principal components as defined in Section 3.1. The number L^{mon} is chosen so that the retained principal components explain at least a given percentage δ^{mon} of the total variability. The statistic T^2 is the standardized squared distance from the center of the orthogonal projection of $\boldsymbol{Z}$ onto the principal component space spanned by $\boldsymbol{\psi}_1^{\mathrm{mon}}, \ldots, \boldsymbol{\psi}_{L^{\mathrm{mon}}}^{\mathrm{mon}}$. Whereas, the distance between $\boldsymbol{Z}$ and its orthogonal projection onto the principal component space is measured through the *SPE* statistic, defined as

$$SPE = ||\boldsymbol{Z} - \hat{\boldsymbol{Z}}||_{\mathbb{H}}^2,$$

where $\hat{\boldsymbol{Z}} = \sum_{l=1}^{L^{\mathrm{mon}}} \xi_l^{\mathrm{mon}} \boldsymbol{\psi}_l^{\mathrm{mon}}$.

Under the assumption of multivariate normality of ξ_l^{mon}, which is approximately true by the central limit theorem (Nomikos and MacGregor 1995), the control limit of the Hotelling's T^2 control chart is obtained as

$$CL_{T^2,\alpha^*} = \frac{L^{\mathrm{mon}}(n-1)(n+1)}{(n-L^{\mathrm{mon}})n} F_{\alpha^*, L^{\mathrm{mon}}, n-L^{\mathrm{mon}}},$$

where $F_{\alpha^*, L^{\mathrm{mon}}, n-L^{\mathrm{mon}}}$ is the $(1-\alpha^*)$-quantile of the Fisher distribution with L^{mon} and $n - L^{\mathrm{mon}}$ degrees of freedom. The control limit for the *SPE* control chart can be computed by using the following equation (Jackson and Mudholkar 1979)

$$CL_{SPE,\alpha^*} = \theta_1 \left[\frac{c_{\alpha^*}\sqrt{2\theta_2 h_0^2}}{\theta_1} + 1 + \frac{\theta_2 h_0 (h_0 - 1)}{\theta_1^2} \right]^{1/h_0},$$

where c_{α^*} is the $(1-\alpha^*)$-quantile of the standard normal distribution, $h_0 = 1 - 2\theta_1\theta_3/3\theta_2^2$, $\theta_j = \sum_{l=L^{\mathrm{mon}}+1}^{\infty} (\lambda_l^{\mathrm{mon}})^j, j = 1, 2, 3$. We use the Šiďak correction $\alpha^* = 1 - (1-\alpha)^{1/2}$ (Šidák 1967) to control the family-wise error rate (FWER) denoted by α.

4. Simulation Study

4.1. Data Generation

The performance of the RoMFCC in identifying mean shifts of the multivariate functional quality characteristic is assessed through a Monte Carlo simulation study. The data are generated similarly to Centofanti et al. (2021) and Chiou, Chen, and Yang (2014). Without loss of generality, the compact domain $\mathcal{T}$ is set equal to $[0, 1]$ and the number of components p is fixed equal to 10. The eigenfunctions $\{\boldsymbol{\psi}_i\}$ are generated by considering the correlation function $\boldsymbol{G}$ through the following steps.

1. Set the diagonal elements $G_{ll}, l = 1, \ldots, p$ of $\boldsymbol{G}$ as the Bessel correlation function of the first kind (Abramowitz and Stegun 1964), that is,

$$G_{ll}(s,t) = (|s-t|\rho/2)^{\nu} \sum_{k=0}^{\infty} \frac{(-(|s-t|\rho)^2/4)^k}{k!\Gamma(\nu + k + 1)},$$

with $\rho = 32$ and $\nu = 0$. Then calculate the eigenvalues $\{\eta_k\}$ and the corresponding eigenfunctions $\{\vartheta_k\}$, $k = 1, 2, \ldots,$ of $G_{ll}, l = 1, \ldots, p$.

2. Obtain the cross-correlation function G_{lj}, $l, j = 1, \ldots, p$ and $l \neq j$, by

$$G_{lj}(t_1, t_2) = \sum_{k=1}^{\infty} \frac{\eta_k}{1 + |l - j|/\rho_{\text{cor}}} \vartheta_k(t_1)\, \vartheta_k(t_2) \quad t_1, t_2 \in \mathcal{T}, \tag{9}$$

where $\rho_{\text{cor}} = 1$.

3. Calculate the eigenvalues $\{\lambda_i\}$ and the corresponding eigenfunctions $\{\boldsymbol{\psi}_i\}$ through the spectral decomposition of $\boldsymbol{G} = \{G_{lj}\}_{l,j=1,\ldots,p}$, for $i = 1, \ldots, L^*$, where $L^* = 225$ is set as the largest integer such that λ_{L^*} is numerically larger than zero.

Let $\boldsymbol{Z} = (Z_1, \ldots, Z_p)$ be

$$\boldsymbol{Z} = \sum_{i=1}^{L^*} \xi_i \boldsymbol{\psi}_i, \tag{10}$$

with $\boldsymbol{\xi}_{L^*} = (\xi_1, \ldots, \xi_{L^*})^T$ generated by means of a multivariate normal distribution with zero mean and covariance $\text{cov}(\boldsymbol{\xi}_{L^*}) = \boldsymbol{\Lambda} = \text{diag}(\lambda_1, \ldots, \lambda_{L^*})$. Furthermore, let the process mean function m be defined by

$$\begin{aligned} m(t) &= 0.2074 + 0.3117 \exp(-371.4 h(t)) \\ &\quad + 0.5284(1 - \exp(0.8217 h(t))) \\ &\quad - 423.3\,[1 + \tanh(-26.15(h(t) + 0.1715))] \quad t \in \mathcal{T}, \end{aligned} \tag{11}$$

where $h(t) = (t - 0.0045)/(0.15 - 0.0045)$. The mean function m is generated to resemble a typical DRC through the phenomenological model presented in Schwab, Senn, and Link (2012). Two different models, namely C_E and C_P, are used to introduce the contamination in the Phase I observations and the mean shift in the Phase II dataset. Specifically, the model C_E, which mimics a splash weld (expulsion) caused by excessive welding current, and the model C_P, which mimics a phase shift of the peak time caused by an excessive electrode force (Xia et al. 2019), are respectively defined as

$$C_E(t) = \begin{cases} -M_E(t - 0.5) & \text{if } t \in [0, 0.5) \\ -2M_E(t - 0.5) & \text{if } t \in [0.5, 1] \end{cases}, \tag{12}$$

and

$$\begin{aligned} C_P(t) &= -m(t) - (M_P/5)t + 0.45(M_P/5) + 0.2074 \\ &\quad + 0.3117 \exp(-371.4 h(t)) + 0.5284(1 - \exp(0.8217 h(t))) \\ &\quad - 423.3\,[1 + \tanh(-26.15(h(t) + 0.1715))] \quad t \in \mathcal{T}, \end{aligned} \tag{13}$$

where $h(t) = (0.0045 + t(0.15 - 0.0045))^{1 + M_P/0.6}$, and M_E and M_P define the shift sizes. Then, the multivariate functional data $\boldsymbol{X} = (X_1, \ldots, X_p)^T$ is obtained as

$$\boldsymbol{X}(t) = \boldsymbol{m}(t) + \boldsymbol{Z}(t)\,\sigma + \boldsymbol{\varepsilon}(t) + B_{CaE}\boldsymbol{C}_E(t) + B_{CaP}\boldsymbol{C}_P(t) \quad t \in \mathcal{T}, \tag{14}$$

where $\boldsymbol{m}$ is a p dimensional vector with components all equal to m, $\sigma = 0.0125$, $\boldsymbol{\varepsilon} = (\varepsilon_1, \ldots, \varepsilon_p)^T$ is a vector of white noise functions such that, for each $t \in [0, 1]$, $\varepsilon_i(t)$ is a normal random variable with zero mean and standard deviation $\sigma_e = 0.0025$. The coefficients B_{CaE} and B_{CaP} are two independent Bernoulli random variables with parameters p_{CaE} and p_{CaP}, respectively. The vectors $\boldsymbol{C}_E = (B_{1,CeE}C_E, \ldots, B_{p,CeE}C_E)^T$ and $\boldsymbol{C}_P = (B_{1,CeP}C_P, \ldots, B_{p,CeP}C_P)^T$ are composed by two sets of independent Bernoulli random variables $\{B_{i,CeE}\}$ and $\{B_{i,CeP}\}$ with parameters p_{CeE} and p_{CeP}, respectively. The generated data are assumed to be discretely observed at 100 equally spaced time points. Three scenarios are considered and referred to as Scenario S1, Scenario S2 and Scenario S3. The Phase I samples of Scenario S1 and Scenario S2 are, respectively, contaminated by functional componentwise and casewise outliers alone, whereas Scenario S3 is contaminated by both componentwise and casewise outliers, respectively. For each contaminated scenario, we consider both contamination models C_E and C_P, referred to as Out-E and Out-P, respectively, and three increasing contamination levels, referred to as C1, C2, and C3. In particular, Scenario S1 and Scenario S2 are obtained by generating data according to (14) with parameters given in Table 1.

In Scenario S3, half of the Phase I dataset is generated according to Scenario S1, while the other half is generated according to Scenario S2. Finally, a further Scenario S0 simulates instead a Phase I sample without any outlier contamination and data are generated with $p_{CaE} = p_{CaP} = p_{CeE} = p_{CeP} = 0$ and $M_E = M_P = 0$. The parameter $\tilde{p}$ in Table 1 is the probability of contamination, which is set equal to 0.05. Supplementary materials C report additional results obtained with $\tilde{p} = 0.1$.

The Phase II sample is generated using (14) with OC conditions corresponding to C_E and C_P and referred to as OC-E and OC-P, respectively. Table 3 provides a summary of the data generation process parameters. For each OC condition setting, we consider two OC patterns, referred to as ONE and ALL, respectively, where either one or all components are anomalous. Each setting is studied at four different severity levels, denoted by $SL = \{1, 2, 3, 4\}$, and with parameters given in Table 2. In the latter, the Bernoulli random variables of (14) are replaced by constant values.

Table 1. Parameters used to generate the Phase I sample in Scenario S1 and Scenario S2 of the simulation study.

	Scenario S1				Scenario S2			
	Out-E		Out-P		Out-E		Out-P	
	$p_{CaE} = p_{CaP} = 1$, $p_{CeE} = \tilde{p}, p_{CeP} = 0$		$p_{CaE} = p_{CaP} = 1$, $p_{CeE} = 0, p_{CeP} = \tilde{p}$		$p_{CaE} = \tilde{p}, p_{CaP} = 0$, $p_{CeE} = p_{CeP} = 1$		$p_{CaE} = 0, p_{CaP} = \tilde{p}$, $p_{CeE} = p_{CeP} = 1$	
	M_E	M_P	M_E	M_P	M_E	M_P	M_E	M_P
C1	0.03	0.00	0.00	0.3375	0.02	0.00	0.00	0.16875
C2	0.045	0.00	0.00	0.425	0.03	0.00	0.00	0.2125
C3	0.06	0.00	0.00	0.50	0.04	0.00	0.00	0.25

Table 2. Parameters used to generate the Phase II sample for OC-E and OC-P and severity level $SL = \{0, 1, 2, 3, 4\}$ in the simulation study.

	ONE				ALL			
	OC-E		OC-P		OC-E		OC-P	
	$B_{CaE} = 1, B_{CaP} = 0,$ $B_{j,CeE} = I(j = 5), B_{j,CeP} = 0$		$B_{CaE} = 0, B_{CaP} = 1,$ $B_{j,CeE} = 0, B_{j,CeP} = I(j = 5)$		$B_{CaE} = 1, B_{CaP} = 0,$ $B_{j,CeE} = 1, B_{j,CeP} = 0$		$B_{CaE} = 0, B_{CaP} = 1,$ $B_{j,CeE} = 0, B_{j,CeP} = 1$	
SL	M_E	M_P	M_E	M_P	M_E	M_P	M_E	M_P
0	0.00	0.00	0.00	0.00	0.00	0.00	0.00	0.00
1	0.015	0.00	0.00	0.25	0.01	0.00	0.00	0.125
2	0.03	0.00	0.00	0.3375	0.02	0.00	0.00	0.16875
3	0.045	0.00	0.00	0.425	0.03	0.00	0.00	0.2125
4	0.06	0.00	0.00	0.50	0.04	0.00	0.00	0.25

Table 3. Phase I generation scenarios and Phase II OC condition settings for the comparison of RoMFCC with competing methods.

	Phase I				Phase II		
Scenario	Phase I contamination type	Contamination probability	Contamination model	Contamination level	OC condition type	OC pattern	SL
S0	No contamination	–	–	–	OC-E, OC-P	ONE, ALL	0, 1, 2, 3, 4
S1	Functional componentwise outliers	0.05, 0.01	Out-E, Out-P	C1, C2, C3	OC-E, OC-P	ONE, ALL	0, 1, 2, 3, 4
S2	Functional casewise outliers	0.05, 0.01	Out-E, Out-P	C1, C2, C3	OC-E, OC-P	ONE, ALL	0, 1, 2, 3, 4
S3	Functional casewise and componentwise outliers	0.05, 0.01	Out-E, Out-P	C1, C2, C3	OC-E, OC-P	ONE, ALL	0, 1, 2, 3, 4

4.2. Simulation Results and Discussion

The proposed RoMFCC framework is compared with several natural competing approaches grouped into control charts for multivariate non-functional and functional data. The first group consists of control charts for multivariate (non-functional) data that are built by summarizing each component of an observation of the multivariate functional quality characteristic with its mean value. the vector of the average of each functional component observation. In this group, we consider (i) the classical *multivariate* Hotelling's T^2 control chart, referred to as MCC; (ii) its *iterative* variant, referred to as iterMCC, where outliers detected by the control chart in Phase I are iteratively removed and control limits are revised until all data are assumed to be IC; (iii) the *multivariate robust* control chart proposed by Chenouri, Steiner, and Variyath (2009) and referred to as RoMCC. As a second group, we consider three approaches that have recently appeared in the profile monitoring literature, namely (iv) the *multivariate functional control chart*, referred to as MFCC, proposed by Capezza et al. (2020); and two variants (v) and (vi), referred to as iterMFCC and OutMFCC, where outliers are (v) *iteratively* removed in Phase I until all data are assumed to be IC or (vi) identified through the *outliergram* for multivariate functional data proposed by Ieva and Paganoni (2020), respectively.

The RoMFCC is implemented as described in Section 3 with $\delta^{fil} = \delta^{imp} = 0.999$ and $\delta^{mon} = 0.7$, and, to take into account the noise increase due to single imputation, three differently imputed datasets are generated through RoMFDI. In supplementary materials C, a sensitivity analysis is performed with respect to δ^{fil}, δ^{imp}, and δ^{mon}. Although the data are observed through noisy discrete values, each component of the generated quality characteristic observations is obtained by (2) with $K = 15$ cubic B-splines estimated through the spline smoothing approach and a roughness penalty on the second derivative (Ramsay and Silverman 2005). For each Phase I sample generation scenario and Phase II OC condition setting reported in Table 3, 50 simulation runs are performed with Phase I sample size of 3000. In particular, for MFCC, iterMFCC, OutMFCC, and RoMFCC, 1000 Phase I observations are used as a training set and the remaining 2000 ones as a tuning set. Additional results for different Phase I sample sizes are provided in supplementary materials C. The Phase II sample is composed of a random sample of 4000 observations. The RoMFCC and the performance of the competing method are assessed in terms of the average run length (ARL), which is defined as the expected number of observations to an OC signal, and is estimated as the inverse of the average proportion, over the simulation runs, of points that fall outside the control limits and is indicated with $\widehat{ARL}$. When $SL = 0$, the $\widehat{ARL}$ is also denoted by $\widehat{ARL}_0$ and must be as close as possible to the reciprocal of the pre-specified FWER α, which is set equal to 0.05 in this simulation study. When $SL \neq 0$, the lower the $\widehat{ARL}$ the better.

Figures 4–7 refer to Scenario S0, Scenario S1, Scenario S2, and Scenario S3, respectively, and display the $\widehat{ARL}$ as a function of the severity level SL, contamination model, contamination level and OC pattern reported in Table 3, with OC condition OC-E and contamination probability $\tilde{p} = 0.05$. Results for the OC condition OC-P are deferred in supplementary materials C.

In Scenario S0, where the Phase I sample is not contaminated by outliers, Figure 4 shows that all the approaches able to account for the functional nature of the data (namely MFCC, iterMFCC, OutMFCC, RoMFCC) achieve the same performance for both OC patterns. Although this scenario should not be favorable for approaches designed to deal with outliers such as iterMFCC, OutMFCC, and RoMFCC, these perform equally to MFCC. All the non-functional approaches (namely MCC, iterMCC, RoMCC) show worse performance than the functional counterparts and no significant differences among themselves.

In Scenario S1, the proposed RoMFCC is shown in Figure 5 to outperform all the competing methods for each contamination model, level, and OC pattern. In particular, the larger

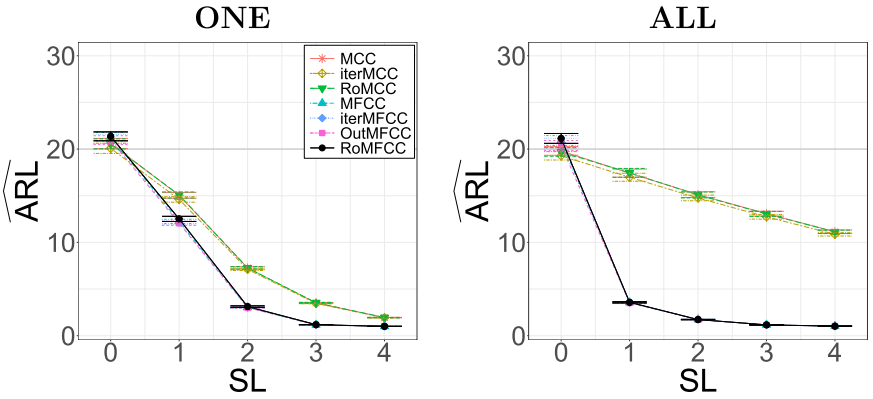

Figure 4. Estimated *ARL* along with ± 2(*standard error*) achieved by MCC, iterMCC, RoMCC, MFCC, iterMFCC, OutMFCC, and RoMFCC for each OC pattern (ONE and ALL) and OC condition OC-E as a function of the severity level *SL* in Scenario S0.

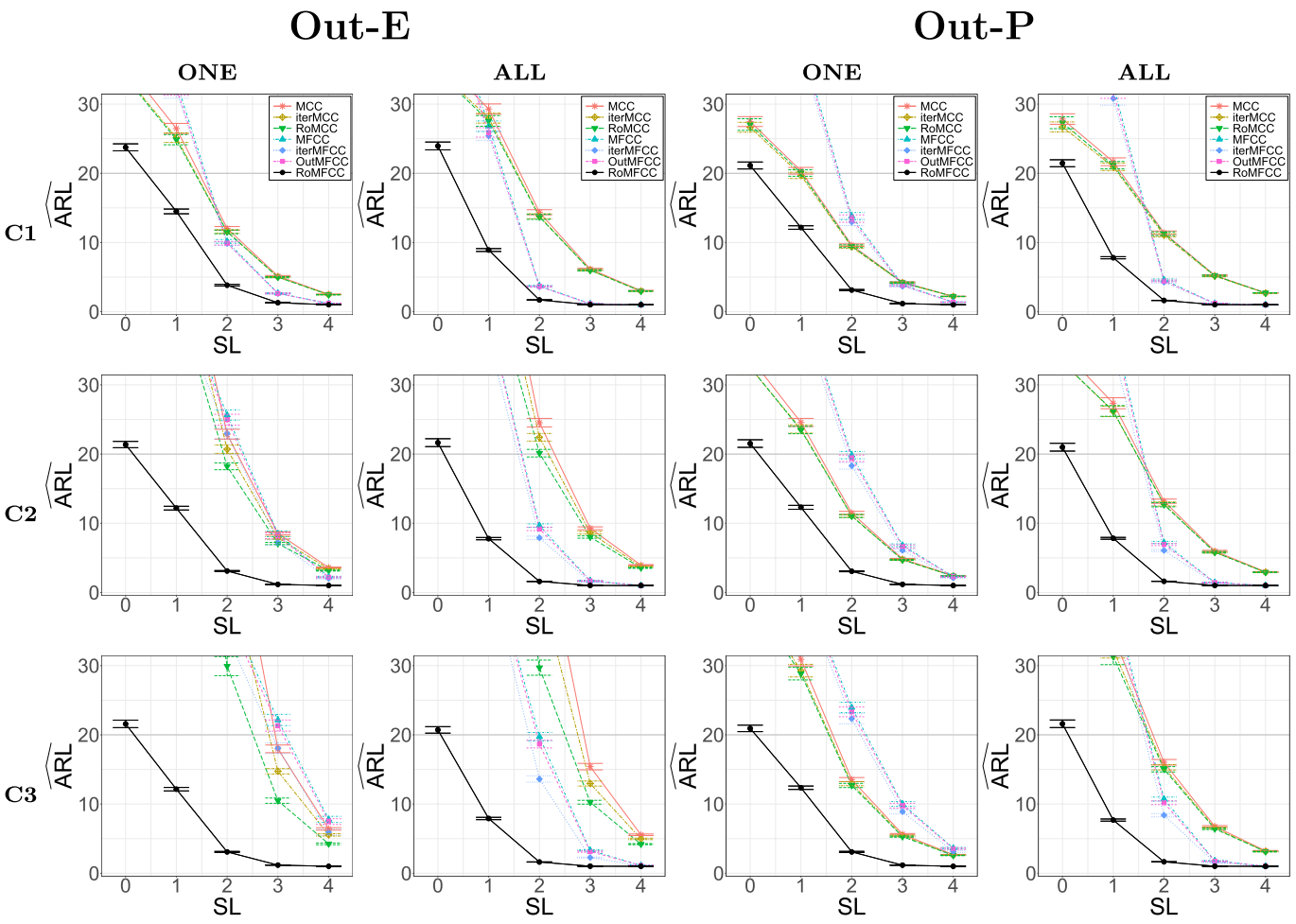

Figure 5. Estimated *ARL* along with ± 2(*standard error*) achieved by MCC, iterMCC, RoMCC, MFCC, iterMFCC, OutMFCC, and RoMFCC for each contamination level (C1, C2, and C3), OC pattern (ONE and ALL) as a function of the severity level *SL* with contamination model Out-E and Out-P and contamination probability 0.05 for OC condition OC-E in Scenario S1.

the contamination level, the better the RoMFCC performance with respect to the competing methods. The RoMFCC performance is indeed almost insensitive to contamination models and levels, while the performance of the competing methods decreases with the contamination level for each contamination model, especially for Out-E. Regarding the non-robust functional methods (namely MFCC and iterMFCC), it turns out that iterMFCC only slightly outperforms MFCC. Moreover, their advantage over non-functional approaches appears only for the OC pattern ALL and decreases with the contamination level. For OC pattern ONE, the non-functional methods outperform the functional counterparts. The unsatisfactory performance of the non-functional methods for the OC pattern ALL reveals their inadequacy in dealing with the functional nature of the data. On the contrary, the rough dimensionality reduction of the non-functional methods results in a better diagnostic performance for OC pattern ONE, that is, when only one component is anomalous.

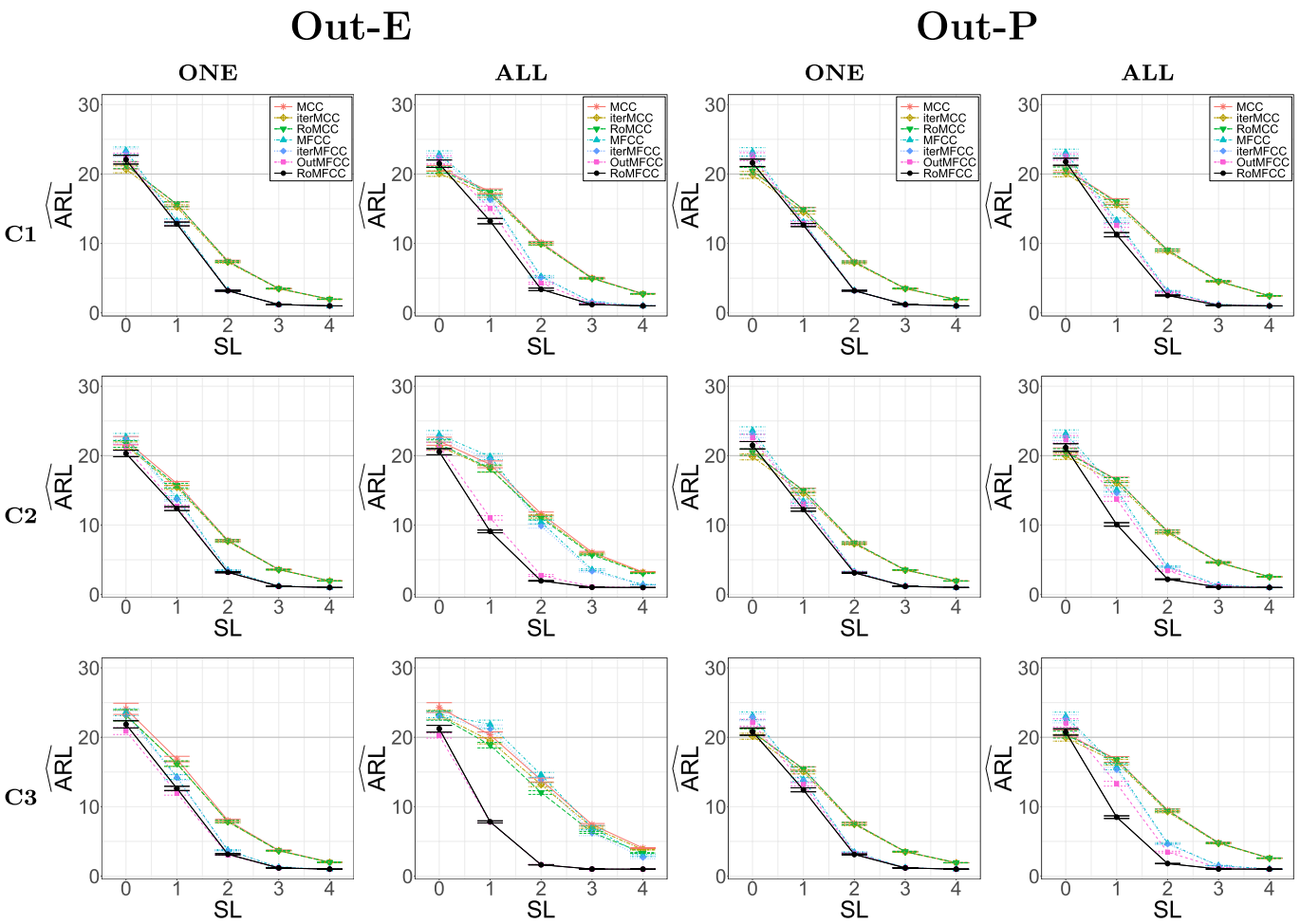

Figure 6. Estimated *ARL* along with ± 2(*standard error*) achieved by MCC, iterMCC, RoMCC, MFCC, iterMFCC, OutMFCC, and RoMFCC for each contamination level (C1, C2, and C3), OC pattern (ONE and ALL) as a function of the severity level *SL* with contamination model Out-E and Out-P and contamination probability $\tilde{p} = 0.05$ for OC condition OC-E in Scenario S2.

Figure 6 shows the RoMFCC as the best method also in Scenario S2, although the performance difference with the competing methods is sometimes less pronounced than in Scenario S1. This is expected because in this scenario the Phase I sample is only contaminated by functional casewise outliers, which is the only contamination type the competing methods are designed to be robust against. Note that the performance of RoMFCC is practically unaffected by outlier contamination also in this scenario.

As Scenario S3 combines elements from both Scenario S1 and Scenario S2, Figure 7 exhibits analogous results to those previously discussed, thereby strengthening the previous findings and underscoring the consistency of the results obtained.

The performance of the RoMFCC is further assessed in supplementary materials C, where additional simulation results are reported whose main findings are briefly summarized below. The RoMFCC is further compared with the competing methods when data are generated with a contamination probability $\tilde{p} = 0.1$. Also in this case, RoMFCC outperforms all the competing methods and performance differences between the proposed and competing methods are less pronounced in Scenario S2 than in Scenario S1. Moreover, the performance of the RoMFCC is studied for the OC condition OC-P and also when the two contamination models, Out-E and Out-P, appear together. Results are coherent with those obtained for OC condition OC-E and in the cases where the contamination model is either Out-E or Out-P.

To investigate the impact of the imputation step of the proposed RoMFDI method on the monitoring performance, RoMFCC is further compared with two methods referred to as *RemAnyComp* and *ImputationMean*. The former removes from the sample all observations with at least a componentwise outlier flagged by the FF, whereas the latter imputes the missing components with the corresponding robust estimate of the functional mean. ImputationMean is not able to guarantee the ARL_0 close to the nominal value, whereas RemAnyComp, by entirely deleting componentwise outliers, may easily lead to an overly small sample size and thus underperforms RoMFCC.

To further underline the importance of being robust against componentwise and casewise functional outliers, the RoMFCC is compared with two simplified versions of it, referred to as *OnlyComp* and *OnlyCase*, respectively. In the former, the FF and RoMFDI steps are followed by a non-robust dimensionality reduction, while, in the latter, the FF step is not performed. Therefore, OnlyComp (resp. OnlyCase) is expected to be resistant to componentwise (resp. casewise) outliers alone. In Scenario S1, OnlyCase achieves the worst performance whereas in Scenario S2, OnlyComp is the worst method. In Scenario S3, OnlyComp performs surprisingly well and is very close to RoMFCC, which however remains the best method. These

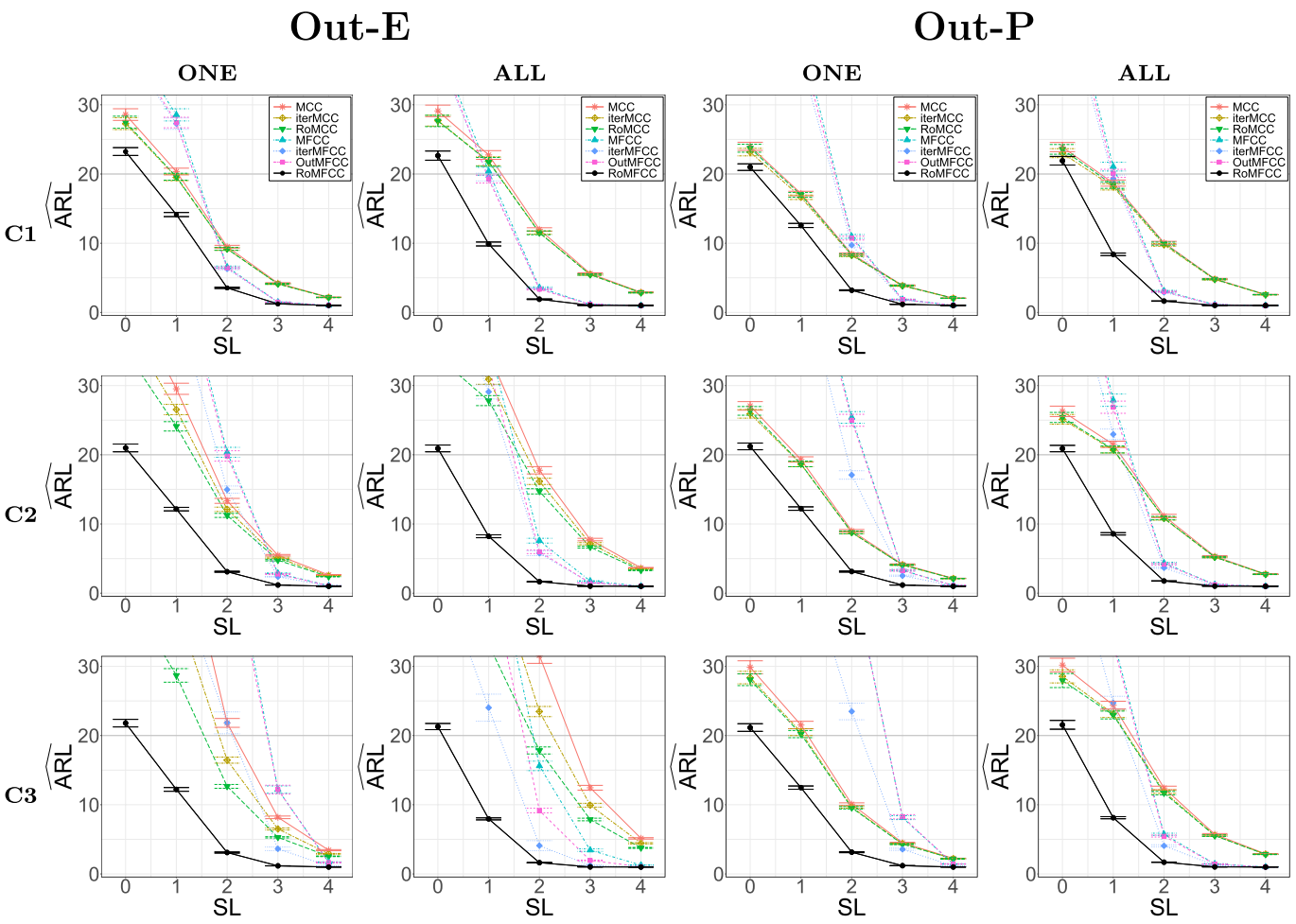

Figure 7. Estimated *ARL* along with ± 2(*standard error*) achieved by MCC, iterMCC, RoMCC, MFCC, iterMFCC, OutMFCC, and RoMFCC for each contamination level (C1, C2, and C3), OC pattern (ONE and ALL) as a function of the severity level *SL* with contamination model Out-E and Out-P and contamination probability $\tilde{p} = 0.05$ for OC condition OC-E in Scenario S3.

additional results bring undoubtedly to the conclusion that there is no superfluous step in the proposed RoMFCC method when, as in the majority of real applications, there is no prior information regarding the presence of casewise and/or componentwise outliers in the Phase I sample.

Then, the sensitivity of the proposed method to the sample size is studied by varying the cardinality of the training and tuning sets. As expected, the larger the sample size, the smaller the $\widehat{ARL}$ achieved by the RoMFCC method.

As mentioned in Section 3, the implementation of RoMFCC relies on the choice of three main parameters, namely δ^{fil}, δ^{imp}, and δ^{mon}, whose sensitivity analysis can be useful to check their influence on the RoMFCC performance. These parameters are found to have a small impact on the RoMFCC performance. Thus, we recommend that practitioners use a large value, say 0.999, for δ^{fil} and δ^{imp} and $\delta^{\text{mon}} = 0.7$, as is typically done in the principal component analysis literature.

Finally, to demonstrate the utility of the functional bivariate filter in the FF, we compare it with its alternative version, referred to as $\text{RoMFCC}_{\text{uni}}$, where only the univariate filter is used in the filtering step. The RoMFCC is found to benefit from a larger dependence among components with respect to $\text{RoMFCC}_{\text{uni}}$, in the identification of functional componentwise outliers.

5. Case Study

To demonstrate the potential of the proposed RoMFCC in real situations, a case study in the automotive industry is presented henceforth. As introduced in Section 1, it addresses the issue of monitoring the quality of the RSW process, which is an autogenous welding process in which two overlapping conventional steel galvanized sheets are joined together, without the use of any filler material (Zhang and Senkara 2011), to guarantee the structural integrity and solidity of the welded items (Martín et al. 2014). Joints are formed by applying pressure to the weld area from two opposite sides through two copper electrodes. The voltage applied to the electrodes generates a current flowing between them through the material. The electrical current flows because the resistance offered by the metals causes significant heat generation (Joule effect) that increases the metal temperature at the faying surfaces of the workpieces up to the melting point. Finally, due to the mechanical pressure of the electrodes, the molten metal of the jointed metal sheets cools and solidifies, forming the so-called weld nugget (Raoelison et al. 2012). Further details on how the typical behavior of a DRC is related to the physical and metallurgical development of a spot weld are provided in Capezza et al. (2021b).

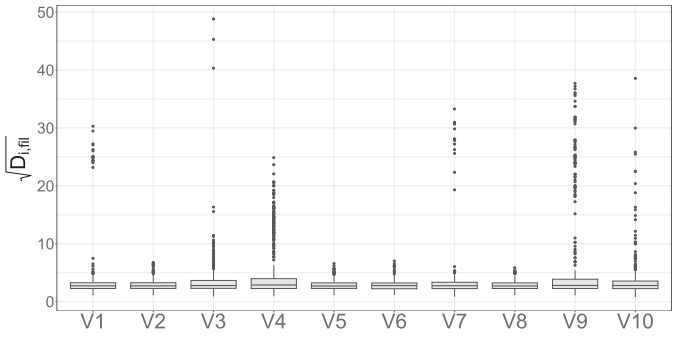

Figure 8. Boxplot of the functional distance square roots $\sqrt{D_{i,fil}}$ (Equation (4)) obtained from the FF applied on the 460 Phase I observations of the training set.

The data analyzed in this study are courtesy of Centro Ricerche Fiat and are recorded during automotive body-in-white lab tests. This stage is generally characterized by a large number of spot welds with different characteristics, for example, the thickness and material of the sheets to be joined together and the welding time. Specifically, this case study focuses on the monitoring of 10 spot welds made by only one welding machine. In particular, for each item, we consider the multivariate functional quality characteristic represented by the vector of 10 DRCs relative to the same 10 spot welding points, normalized in the time domain $[0, 1]$. The dataset contains a total number of 1839 items and resistance measurements were collected at a regular grid of points equally spaced by 1 ms.

The RSW process quality is directly affected by electrode wear that leads to changes in electrical, thermal, and mechanical contact conditions at electrode and metal sheet interfaces (Manladan et al. 2017). For this reason, electrodes are subjected to periodical tip dressing. Thus, a critical issue is the swift identification of DRC mean shifts caused by electrode wear as a criterion to guide the electrode tip dressing program. To this aim, 919 observations of the multivariate functional quality characteristic corresponding to spot welds made immediately before electrode tip dressing are used to form the Phase I sample. The remaining 920 observations are used in Phase II to compare the in-line monitoring performance of the proposed RoMFCC with that of competing methods. The RoMFCC is implemented as in Section 4, where 460 Phase I observations, which are randomly selected without remittance, are used to form the training set and the remaining 459 ones for the tuning set. Figure 8 shows the boxplot of the functional distance square root $\sqrt{D_{i,fil}}$ (Equation (4)) obtained from the functional univariate filter applied on the 460 Phase I observations of the training set. This figure confirms the outlier contamination in the training set, as already illustrated by Figure 1 for 100 randomly sampled DRCs.

Figure 9 shows the Hotelling's T^2 and *SPE* control charts of the RoMFCC framework for the case study dataset. The vertical line separates the monitoring statistics calculated for the tuning set, on the left, and the Phase II sample on the right, while the control limits are shown as horizontal lines. Note that the number of tuning-set observations that plot above the control limits is expected because these points may include functional casewise outliers not filtered out by the FF. In Phase II, the RoMFCC signals 72% of the observations as OC, which reflects the performance of the proposed method in tracking mean shifts caused by electrode wear.

Table 4. Estimated ARL values, denoted as $\widehat{ARL}$, on the Phase II sample, mean of the empirical bootstrap distribution of $\widehat{ARL}$, denoted by $\overline{\widehat{ARL}}$, and the corresponding bootstrap 95% confidence interval (CI) for each monitoring method.

		$\widehat{ARL}$	$\overline{\widehat{ARL}}$	CI
Non-functional	MCC	2.977	2.993	[2.714,3.281]
	iterMCC	2.165	2.171	[2.015,2.337]
	RoMCC	1.652	1.655	[1.559,1.739]
Functional	MFCC	1.885	1.892	[1.783,1.998]
	iterMFCC	1.603	1.605	[1.519,1.702]
	OutMFCC	1.800	1.807	[1.708,1.911]
	RoMFCC	1.390	1.391	[1.327,1.459]

Finally, the proposed method is compared with the competing methods presented in the simulation study of Section 4 through the estimated ARL, denoted as $\widehat{ARL}$, in the Phase II sample, as shown in Table 4. As expected from the results in Section 4, the considered non-functional approaches (MCC, iterMCC, and RoMCC) show worse performance than the functional counterparts (MFCC, iterMFCC, OutMFCC, and RoMFCC) because they are not able to satisfactorily capture the functional nature of the data, apart from RoMCC that achieves a smaller ARL with respect to MFCC. Moreover, robust approaches (RoMCC and RoMFCC) outperform their non-robust counterparts, that is, the $\widehat{ARL}$ achieved by RoMCC is smaller than MCC and iterMCC, whereas the $\widehat{ARL}$ achieved by RoMFCC is smaller than MFCC and iterMFCC. The uncertainty of $\widehat{ARL}$ is quantified through a bootstrap analysis (Efron and Tibshirani 1994). Table 4 reports the mean of the empirical bootstrap distribution of $\widehat{ARL}$, denoted by $\overline{\widehat{ARL}}$, and the corresponding bootstrap 95% confidence interval (CI) for each monitoring method. Bootstrap 95% CIs achieved by the RoMFCC are strictly below those of all considered monitoring approaches. Therefore, the proposed RoMFCC stands out as the best method to promptly identify OC conditions in the considered RWS process characterized by a Phase I sample contaminated by functional outliers.

6. Conclusions

In this article, we propose a new robust framework for the statistical process monitoring of multivariate functional data, referred to as robust multivariate functional control chart (RoMFCC).

The RoMFCC is the first statistical process monitoring (SPM) framework for multivariate functional quality characteristics that is robust to both functional casewise and componentwise outliers. Indeed, methods already present in the literature either apply robust approaches to multivariate scalar features extracted from the profiles or use diagnostic approaches on the multivariate functional data to iteratively remove outliers. However, the former are not able to capture the functional nature of the data, while the latter are not able to deal with functional componentwise outliers. The novelty of the proposed RoMFCC lies both in its characteristic features, which are novel approaches in the functional data analysis literature and their combination.

The performance of the RoMFCC framework is assessed through an extensive Monte Carlo simulation study and is compared with several monitoring methods for multivariate scalar data and multivariate functional data already appeared in the literature. The ability to estimate the distribution of the data

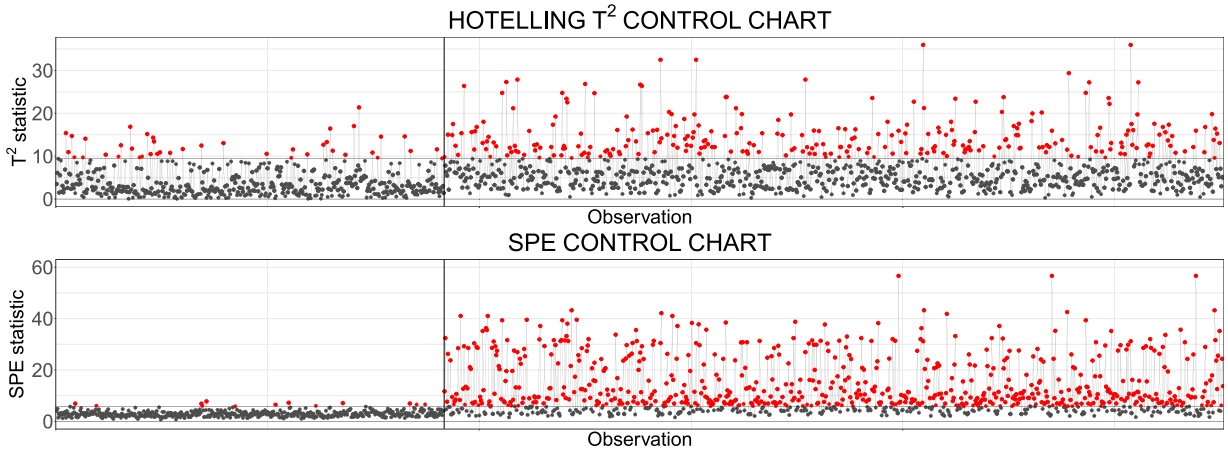

Figure 9. Hotelling's T^2 and *SPE* control charts of the RoMFCC framework for the case study dataset. The vertical line separates the monitoring statistics calculated for the tuning set, on the left, and the Phase II sample, on the right, while the control limits are shown as horizontal lines.

without removing observations allows the RoMFCC to outperform the competitors in all the considered settings and to represent the only alternative in high-dimensional scenarios where most of the competing methods may even fail. The proposed method is suitable for monitoring industrial processes where many functional variables are available and possibly contaminated by outliers, such as anomalies in data acquisition and data collected during a fault in the process.

The practical applicability of the proposed method is illustrated through the case study that motivated this research and addressed the issue of monitoring the quality of a resistance spot-welding (RSW) process in the automotive industry through multivariate observations of the dynamic resistance curves as the quality characteristic of interest. Also in this case study, the RoMFCC outperforms all competitors considered in the identification of the out-of-control state of the RSW process due to the excessive wear of the electrode used.

Supplementary Materials

The supplementary material contains a brief description of the equivariant functional *M*-estimator and the functional normalized median absolute deviation estimators (A), the proof of Proposition 1 (B), additional simulation results (C), as well as the R code to reproduce graphics and results over competing methods in the simulation study. The R code is also available at *https://www.sfere.unina.it/publications/*.

Acknowledgments

The authors are deeply grateful to the editor, the associate editor, and three referees for their reviews, which led to significant improvement of the article. This article reflects only the authors' views and opinions, neither the European Union nor the European Commission can be considered responsible for them.

Disclosure Statement

The authors report there are no competing interests to declare.

Funding

The research activity of A. Lepore and F. Centofanti were carried out within the MICS (Made in Italy - Circular and Sustainable) Extended Partnership and received funding from the European Union Next-GenerationEU (PIANO NAZIONALE DI RIPRESA E RESILIENZA (PNRR) - MISSIONE 4 COMPONENTE 2, INVESTIMENTO 1.3 - D.D. 1551.11-10-2022, PE00000004). The research activity of B. Palumbo was carried out within the MOST - Sustainable Mobility National Research Center and received funding from the European Union Next-GenerationEU (PIANO NAZIONALE DI RIPRESA E RESILIENZA (PNRR) - MISSIONE 4 COMPONENTE 2, INVESTIMENTO 1.4 - D.D. 1033.17-06-2022, CN00000023). This manuscript reflects only the authors' views and opinions, neither the European Union nor the European Commission can be considered responsible for them.

ORCID

Christian Capezza https://orcid.org/0000-0002-8358-4800
Fabio Centofanti https://orcid.org/0000-0002-5007-525X
Antonio Lepore https://orcid.org/0000-0002-8739-5310
Biagio Palumbo https://orcid.org/0000-0003-1036-8127

References

Abramowitz, M., and Stegun, I. A. (1964), *Handbook of Mathematical Functions: With Formulas, Graphs, and Mathematical Tables*, (Vol. 55), U.S. Government Printing Office. [538]

Agostinelli, C., Leung, A., Yohai, V. J., and Zamar, R. H. (2015), "Robust Estimation of Multivariate Location and Scatter in the Presence of Cellwise and Casewise Contamination," *Test*, 24, 441–461. [533,535,536]

Alemán-Gómez, Y., Arribas-Gil, A., Desco, M., Elías, A., and Romo, J. (2022), "Depthgram: Visualizing Outliers in High-Dimensional Functional Data with Application to fMRI Data Exploration," *Statistics in Medicine*, 41, 2005–2024. [533]

Alfaro, J., and Ortega, J. F. (2009), "A Comparison of Robust Alternatives to Hotelling's T^2 Control Chart," *Journal of Applied Statistics*, 36, 1385–1396. [532]

Alqallaf, F., Van Aelst, S., Yohai, V. J., and Zamar, R. H. (2009), "Propagation of Outliers in Multivariate Data," *The Annals of Statistics*, 37, 311–331. [533,534]

Arribas-Gil, A., and Romo, J. (2014), "Shape Outlier Detection and Visualization for Functional Data: The Outliergram," *Biostatistics*, 15, 603–619. [533]

Boente, G., and Salibián-Barrera, M. (2021), "Robust Functional Principal Components for Sparse Longitudinal Data," *Metron*, 79, 159–188. [533]

Branden, K. V., and Verboven, S. (2009), "Robust Data Imputation," *Computational Biology and Chemistry*, 33, 7–13. [533,535,537,538]

Cabana, E., and Lillo, R. E. (2022), "Robust Multivariate Control Chart based on Shrinkage for Individual Observations," *Journal of Quality Technology*, 54, 415–440. [532]

Capezza, C., Centofanti, F., Lepore, A., Menafoglio, A., Palumbo, B., and Vantini, S. (2021a), "Functional Regression Control Chart for Monitoring Ship CO_2 Emissions," *Quality and Reliability Engineering International*, 38, 1519–1537. [531,533]

Capezza, C., Centofanti, F., Lepore, A., Menafoglio, A., Palumbo, B., and Vantini, S. (2023), "funcharts: Control Charts for Multivariate Functional Data in R, *Journal of Quality Technology*, 55, 566–583. [531,533,535]

Capezza, C., Centofanti, F., Lepore, A., Menafoglio, A., Palumbo, B., and Vantini, S. (2024), *funcharts: Functional Control Charts*, R package version 1.4.1. [533]

Capezza, C., Centofanti, F., Lepore, A., and Palumbo, B. (2021b), "Functional Clustering Methods for Resistance Spot Welding Process Data in the Automotive Industry," *Applied Stochastic Models in Business and Industry*, 37, 908–925. [531,543]

Capezza, C., Lepore, A., Menafoglio, A., Palumbo, B., and Vantini, S. (2020), "Control Charts for Monitoring Ship Operating Conditions and CO_2 Emissions based on Scalar-on-Function Regression," *Applied Stochastic Models in Business and Industry*, 36, 477–500. [531,533,540]

Centofanti, F., Colosimo, B. M., Grasso, M. L., Menafoglio, A., Palumbo, B., and Vantini, S. (2023), "Robust Functional ANOVA with Application to Additive Manufacturing," *Journal of the Royal Statistical Society*, Series C, 72, 1210–1234. [532,536]

Centofanti, F., Lepore, A., Kulahci, M., and Spooner, M. P. (2022), "Real-Time Monitoring of Functional Data," arXiv preprint arXiv:2205.06256. [531]

Centofanti, F., Lepore, A., Menafoglio, A., Palumbo, B., and Vantini, S. (2021), "Functional Regression Control Chart," *Technometrics*, 63, 281–294. [531,533,535,538]

Chenouri, S., Steiner, S. H., and Variyath, A. M. (2009), "A Multivariate Robust Control Chart for Individual Observations," *Journal of Quality Technology*, 41, 259–271. [532,540]

Chiou, J.-M., Chen, Y.-T., and Yang, Y.-F. (2014), "Multivariate Functional Principal Component Analysis: A Normalization Approach," *Statistica Sinica*, 24, 1571–1596. [535,536,538]

Cuesta-Albertos, J. A., and Fraiman, R. (2006), "Impartial Trimmed Means for Functional Data," *DIMACS Series in Discrete Mathematics and Theoretical Computer Science*, 72, 121. [532]

Cuevas, A., and Fraiman, R. (2009), "On Depth Measures and Dual Statistics. A Methodology for Dealing with General Data," *Journal of Multivariate Analysis*, 100, 753–766. [532]

Dickinson, D., Franklin, J., Stanya, A., et al. (1980), "Characterization of Spot Welding Behavior by Dynamic Electrical Parameter Monitoring," *Welding Journal*, 59, 170. [531]

Efron, B., and Tibshirani, R. J. (1994), *An Introduction to the Bootstrap*, Boca Raton, FL: CRC Press. [544]

Fraiman, R., and Muniz, G. (2001), "Trimmed Means for Functional Data," *Test*, 10, 419–440. [532]

Grasso, M., Menafoglio, A., Colosimo, B. M., and Secchi, P. (2016), "Using Curve-Registration Information for Profile Monitoring," *Journal of Quality Technology*, 48, 99–127. [533]

Happ, C., and Greven, S. (2018), "Multivariate Functional Principal Component Analysis for Data Observed on Different (Dimensional) Domains," *Journal of the American Statistical Association*, 113, 649–659. [535]

Hubert, M., Rousseeuw, P. J., and Segaert, P. (2015), "Multivariate Functional Outlier Detection," *Statistical Methods & Applications*, 24, 177–202. [532,533]

Hubert, M., Rousseeuw, P. J., and Vanden Branden, K. (2005), "ROBPCA: A New Approach to Robust Principal Component Analysis," *Technometrics*, 47, 64–79. [533,536]

Hyndman, R. J., and Shang, H. L. (2010), "Rainbow Plots, Bagplots, and Boxplots for Functional Data," *Journal of Computational and Graphical Statistics*, 19, 29–45. [533]

Hyndman, R. J., and Ullah, M. S. (2007), "Robust Forecasting of Mortality and Fertility Rates: A Functional Data Approach," *Computational Statistics & Data Analysis*, 51, 4942–4956. [533]

Ieva, F., and Paganoni, A. M. (2020), "Component-Wise Outlier Detection Methods for Robustifying Multivariate Functional Samples," *Statistical Papers*, 61, 595–614. [533,540]

Jackson, J. E., and Mudholkar, G. S. (1979), "Control Procedures for Residuals Associated with Principal Component Analysis," *Technometrics*, 21, 341–349. [538]

Jensen, W. A., Birch, J. B., and Woodall, W. H. (2007), "High Breakdown Estimation Methods for Phase I Multivariate Control Charts," *Quality and Reliability Engineering International*, 23, 615–629. [532]

Jolliffe, I. (2011), *Principal Component Analysis*, New York: Springer. [536]

Kokoszka, P., and Reimherr, M. (2017), *Introduction to Functional Data Analysis*, Chapman and Hall/CRC. [531]

Kordestani, M., Hassanvand, F., Samimi, Y., and Shahriari, H. (2020), "Monitoring Multivariate Simple Linear Profiles Using Robust Estimators," *Communications in Statistics-Theory and Methods*, 49, 2964–2989. [532]

Kruger, U., and Xie, L. (2012), *Statistical Monitoring of Complex Multivatiate Processes: With Applications in Industrial Process Control*, Chichester: Wiley. [532,535]

Lee, S., Shin, H., and Billor, N. (2013), "M-type Smoothing Spline Estimators for Principal Functions," *Computational Statistics & Data Analysis*, 66, 89–100. [533]

Leung, A., Yohai, V., and Zamar, R. (2017), "Multivariate Location and Scatter Matrix Estimation Under Cellwise and Casewise Contamination," *Computational Statistics & Data Analysis*, 111, 59–76. [533,535,536,537]

Little, R. J., and Rubin, D. B. (2019), *Statistical Analysis with Missing Data*, Hoboken, NJ: Wiley. [538]

Locantore, N., Marron, J., Simpson, D., Tripoli, N., Zhang, J., Cohen, K., Boente, G., Fraiman, R., Brumback, B., Croux, C., et al. (1999), "Robust Principal Component Analysis for Functional Data," *Test*, 8, 1–73. [533]

López-Pintado, S., and Romo, J. (2011), "A Half-Region Depth for Functional Data," *Computational Statistics & Data Analysis*, 55, 1679–1695. [532]

Manladan, S., Yusof, F., Ramesh, S., Fadzil, M., Luo, Z., and Ao, S. (2017), "A Review on Resistance Spot Welding of Aluminum Alloys," *The International Journal of Advanced Manufacturing Technology*, 90, 605–634. [544]

Maronna, R. A., Martin, R. D., Yohai, V. J., and Salibián-Barrera, M. (2019), *Robust Statistics: Theory and Methods (with R)*, Hoboken, NJ: Wiley. [532,534,536]

Martín, Ó., Pereda, M., Santos, J. I., and Galán, J. M. (2014), "Assessment of Resistance Spot Welding Quality based on Ultrasonic Testing and Tree-based Techniques," *Journal of Materials Processing Technology*, 214, 2478–2487. [531,543]

Menafoglio, A., Grasso, M., Secchi, P., and Colosimo, B. M. (2018), "Profile Monitoring of Probability Density Functions via Simplicial Functional PCA with Application to Image Data," *Technometrics*, 60, 497–510. [531]

Moheghi, H., Noorossana, R., and Ahmadi, O. (2022), "Phase I and Phase II Analysis of Linear Profile Monitoring Using Robust Estimators," *Communications in Statistics-Theory and Methods*, 51, 1252–1269. [532]

Montgomery, D. C. (2012), *Introduction to Statistical Quality Control*, Hoboken, NJ: Wiley. [531]

Nomikos, P., and MacGregor, J. F. (1995), "Multivariate SPC Charts for Monitoring Batch Processes," *Technometrics*, 37, 41–59. [538]

Noorossana, R., Saghaei, A., and Amiri, A. (2011), *Statistical Analysis of Profile Monitoring*, Hoboken, NJ: Wiley. [531,533]

R Core Team. (2021), *R: A Language and Environment for Statistical Computing*, Vienna, Austria: R Foundation for Statistical Computing. [533]

Ramaker, H.-J., van Sprang, E. N., Westerhuis, J. A., and Smilde, A. K. (2004), "The Effect of the Size of the Training Set and Number of Principal Components on the False Alarm Rate in Statistical Process Monitoring," *Chemometrics and Intelligent Laboratory Systems*, 73, 181–187. [535]

Ramsay, J. O., and Silverman, B. W. (2005), *Functional Data Analysis*, New York: Springer. [531,536,540]

Raoelison, R., Fuentes, A., Rogeon, P., Carre, P., Loulou, T., Carron, D., and Dechalotte, F. (2012), "Contact Conditions on Nugget Development During Resistance Spot Welding of Zn Coated Steel Sheets Using Rounded Tip Electrodes," *Journal of Materials Processing Technology*, 212, 1663–1669. [543]

Rocke, D. M. (1996), "Robustness Properties of S-estimators of Multivariate Location and Shape in High Dimension," *The Annals of Statistics*, 24, 1327–1345. [538]

Rousseeuw, P. J. (1984), "Least Median of Squares Regression," *Journal of the American statistical association*, 79, 871–880. [532]

Rousseeuw, P. J., and Bossche, W. V. D. (2018), "Detecting Deviating Data Cells," *Technometrics*, 60, 135–145. [533]

Sawant, P., Billor, N., and Shin, H. (2012), "Functional Outlier Detection with Robust Functional Principal Component Analysis," *Computational Statistics*, 27, 83–102. [533,536]

Schwab, I., Senn, M., and Link, N. (2012), "Improving Expert Knowledge in Dynamic Process Monitoring by Symbolic Regression," in *2012 Sixth International Conference on Genetic and Evolutionary Computing*, pp. 132–135. IEEE. [539]

Šidák, Z. (1967), "Rectangular Confidence Regions for the Means of Multivariate Normal Distributions," *Journal of the American Statistical Association*, 62, 626–633. [538]

Sinova, B., Gonzalez-Rodriguez, G., and Van Aelst, S. (2018), "M-estimators of Location for Functional Data," *Bernoulli*, 24, 2328–2357. [532]

Tarr, G., Müller, S., and Weber, N. C. (2016), "Robust Estimation of Precision Matrices Under Cellwise Contamination," *Computational Statistics & Data Analysis*, 93, 404–420. [533]

Van Buuren, S. (2018), *Flexible Imputation of Missing Data*, Boca Raton, FL: CRC Press. [538]

Van Ginkel, J. R., Van der Ark, L. A., Sijtsma, K., and Vermunt, J. K. (2007), "Two-Way Imputation: A Bayesian Method for Estimating Missing Scores in Tests and Questionnaires, and an Accurate Approximation," *Computational Statistics & Data Analysis*, 51, 4013–4027. [538]

Vargas, N. J. A. (2003), "Robust Estimation in Multivariate Control Charts for Individual Observations," *Journal of Quality Technology*, 35, 367–376. [532]

Xia, Y.-J., Su, Z.-W., Li, Y.-B., Zhou, L., and Shen, Y. (2019), "Online Quantitative Evaluation of Expulsion in Resistance Spot Welding," *Journal of Manufacturing Processes*, 46, 34–43. [539]

Zhang, H., and Senkara, J. (2011), *Resistance Welding: Fundamentals and Applications*, Boca Raton, FL: CRC Press. [543]